Journal of Radiation Research, Vol. 59, No. 3, 2018, pp. 338–380
doi: 10.1093/jrr/rry024
Advance Access Publication: 5 April 2018

VK-phantom male with 583 structures and female with 459 structures, based on the sectioned images of a male and a female, for computational dosimetry

Jin Seo Park[1], Yong Wook Jung[1], Hyung-Do Choi[2] and Ae-Kyoung Lee[2,*]

[1]Department of Anatomy, Dongguk University School of Medicine, 87 Dongdae-ro, Gyeongju-si 38066, Republic of Korea
[2]Radio & Satellite Research Division, Broadcasting & Media Research Laboratory, Electronics and Telecommunications Research Institute (ETRI), 218 Gajeong-ro, Yuseong-gu, Daejeon 34129, Republic of Korea
*Corresponding author: Radio & Satellite Research Division, Broadcasting & Media Research Laboratory, Electronics and Telecommunications Research Institute (ETRI), 218 Gajeong-ro, Yuseong-gu, Daejeon 34129, Republic of Korea. Tel/Fax: +82-42-860-4971. Email: aklee@etri.re.kr
(Received 24 August 2017; revised 9 November 2017; editorial decision 3 March 2018)

ABSTRACT

The anatomical structures in most phantoms are classified according to tissue properties rather than according to their detailed structures, because the tissue properties, not the detailed structures, are what is considered important. However, if a phantom does not have detailed structures, the phantom will be unreliable because different tissues can be regarded as the same. Thus, we produced the Visible Korean (VK) -phantoms with detailed structures (male, 583 structures; female, 459 structures) based on segmented images of the whole male body (interval, 1.0 mm; pixel size, 1.0 mm^2) and the whole female body (interval, 1.0 mm; pixel size, 1.0 mm^2), using house-developed software to analyze the text string and voxel information for each of the structures. The density of each structure in the VK-phantom was calculated based on Virtual Population and a publication of the International Commission on Radiological Protection. In the future, we will standardize the size of each structure in the VK-phantoms. If the VK-phantoms are standardized and the mass density of each structure is precisely known, researchers will be able to measure the exact absorption rate of electromagnetic radiation in specific organs and tissues of the whole body.

Keywords: electromagnetic radiation; radiometry; phantoms imaging; Visible Human Project

INTRODUCTION

To investigate the human body's absorption of electromagnetic ionizing and non-ionizing radiation generated by electronic and medical devices, various computational dosimetry phantoms of humans have been developed based on magnetic resonance imaging (MRI), computed tomography (CT) [1, 2], sectioned images [3–6] and hybrid images [7, 8].

However, in most phantoms, detailed structures of the entire body cannot be shown due to the limited resolution of CT or MRI. Even the International Commission on Radiological Protection (ICRP) and Virtual Family reference phantoms (which were generated from various source images, including high-resolution sectioned images and hybrid images) contain only 137 structures and 103 structures for the whole human body, respectively [1, 9–11]. The reasons that detailed structures could not be shown in the phantoms were as follows. First, the structures in the source images were not segmented in detail, even though detailed structures could be observed in the source images. Second, the voxel size of the source images was too large (<2 mm^3), despite the source images with very small voxel size <0.2 mm^3). Third, an increase in the number of structures in the phantom resulted in a large file size, meaning that the phantom could not be examined on a personal computer. In particular, in the case of phantoms based on polygonal surface models, a huge file and an enormous number of polygonal surfaces were made, and consequently, the phantom could not be managed by researchers or workers for a commercial test.

Furthermore, in Virtual Population [11], which contains the most well-known phantom data, phantom structures are classified only according to the tissue features based on the Gabriel List [12], though this can lead to erroneous measurement results because tissues with identical features can be interpreted as different, and

tissues with different features can be interpreted as being identical. For example, in the ICRP reference phantom, the densities of the esophagus, spinal cord, and trachea are identical [9, 13, 14], but their tissue features differ: the esophagus is composed of muscle tissue, the spinal cord is composed of nerve tissue, and the trachea is composed of cartilaginous tissue. In the case of Virtual Population, the density of the cerebellum (nerve tissue), esophagus (muscle tissue) and urinary bladder (connective tissue) are considered to be identical [1], but their tissue features differ.

The aim of the current study was to present the Visible Korean (VK) phantom with 583 (male) and 459 (female) structures with sufficient segmentation such that radiation energy absorption can be evaluated. Another aim was to develop methods for converting large-sized segmentation data into a phantom. To achieve these goals, phantoms of a precise shape and detailed structures were manufactured based on high-resolution, real-color sectioned images of the VK.

MATERIALS AND METHODS

In previous studies, 8590 sectioned images of a whole male body (intervals, 0.2 mm; pixel size, 0.2 mm^2; resolution, 3040 × 2008; color depth, 24 bit color; file format, TIF) [15] and 4116 sectioned images of a whole female body [intervals, 0.2 mm (head to pelvis) or 1.0 mm (lower limb); pixel size, 0.1 mm^2; resolution, 5616 × 3744; color depth, 48 bit color; file format, BMP] [16] were produced. In the male and female images, real color and high-resolution structures could be observed in the cross-sectional plane (Fig. 1a and c; Table 1).

We used the data of previous studies, which were for segmented images with 583 structures in the male body (resolution, 2468 × 1407; interval, 1 mm; pixel size, 0.2 mm^2) (Table 2) [17] and segmented images with 171 structures in the female body (resolution, 5610 × 2300; interval, 1 mm; pixel size, 0.1 mm^2) (Table 3) [16] based on the sectioned images of a male and female. In this study, to make a female phantom containing more detailed structures, additional segmentation was performed as follows. First, to segment the sectioned images of the female, the selected structures were outlined using the Quick Selection Tool or the Magnetic Lasso Tool in Photoshop CC 2015 (Adobe Systems, Inc., San Jose, CA, USA). The inner areas of the outlines were filled with specific RGB colors and saved as the segmented images (Fig. 1b and d; Table 1) [18, 19]. Consequently, we also generated segmented images containing an additional 288 structures from the female sectioned images to generate a total of 459 structures (Table 3).

The pixel size of the segmented images (both male and female) was increased from 0.2 mm^2 (male) or 0.1 mm^2 (female) to 1 mm^2 (resolution of male, 493 × 281; resolution of female, 562 × 230). Consequently, the voxels of the segmented images became 1-mm^3 cubes, and the file size of the images decreased from 16.5 GB to 675 MB for males and from 59.2 GB to 608 MB for females (Table 1).

To produce a phantom of TXT format, house-developed software (VK-phantom.jar) was designed using Java language on Eclipse Java IDE for web developers, Luna Service Release 1 (4.4.1). In the software, all voxel information (pixels, intervals, and RGB colors) of each structure in the segmented images could be converted into numerical data in TXT format.

After identification (ID) numbers were serially assigned to all segmented structures in the segmented images, the ID numbers and RGB values of segmented structures were recorded in data.xlsx (Fig. 2a). The data.xlsx was converted into data.txt. When the segmented images of male and data.txt were opened on VK-phantom.jar, the *x*, *y* and *z* coordinates and RGB values were stored temporarily on a personal computer, and the RGB values in the segmented

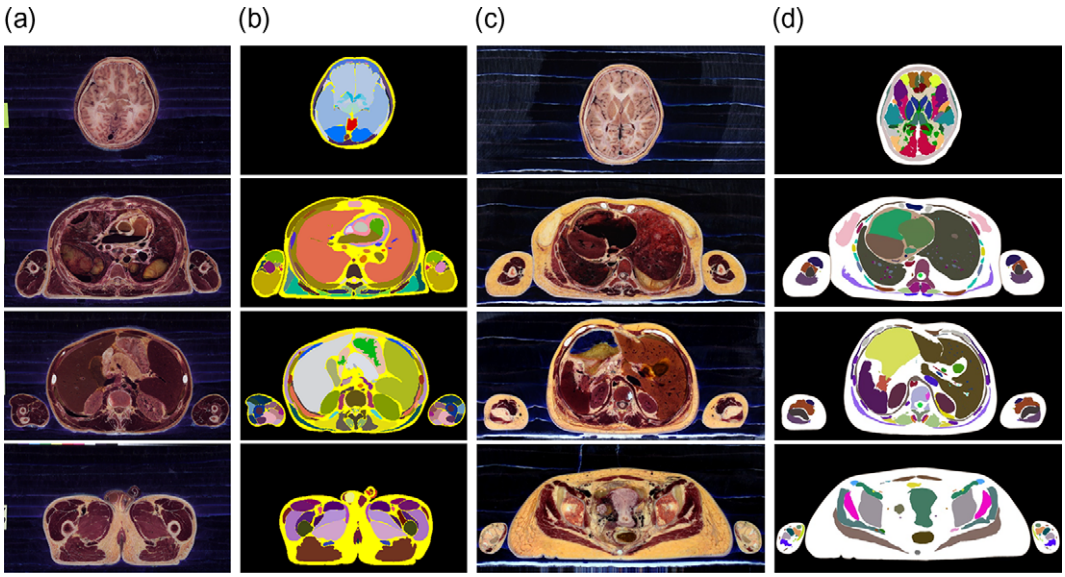

Fig. 1. Sectioned images and segmented images of a male and female for making VK-phantoms. (a) In the sectioned images of the male whole body, (b) segmented images of 583 structures were made. (c) In the sectioned images of the female whole body, (d) segmented images of 459 structures were made.

Table 1. Features of the segmented images and male and female VK-phantoms

Sex	Images	Number of structures	Number of data	Intervals (mm)	Pixel or voxel size	Color depth (bit color)	Total file size (GB)	File format
Male	Sectioned images[a]		8500	0.2	0.2 mm^2 (pixel)	24	82.5	TIFF
	Segmented images[a]	581	1700	1.0	0.2 mm^2 (pixel)	24	16.5	TIFF
	VK-phantom	581	1		1.0 mm^3 (voxel)		1.9	TXT
Female	Sectioned images[a]		4116	0.2[b] or 1.0[c]	0.1 mm^2 (pixel)	48	580.0	TIFF
	Segmented images[a]	171	1643	1.0	0.1 mm^2 (pixel)	24	59.2	TIFF
	Segmented images	287		1.0	0.1 mm^2 (pixel)	24	59.2	TIFF
	VK-phantom	458	1		1.0 mm^3 (voxel)		0.9	TXT

[a]Result of a previous study.
[b]Upper body from the head to perineum.
[c]Lower limb from below the perineum to the sole.

images were converted into ID numbers (Fig. 2b). Finally, the *x*, *y* and *z* coordinates and ID numbers were saved as the VK-phantom male in TXT format. Voxel information for the male VK-phantom, including the *x*, *y* and *z* coordinates and ID number, are presented in a row (Fig. 2c). The VK-phantom female (in TXT format) was generated from the segmented images of the female using the same methods.

To analyze the text string in the VK-phantom of TXT format, house-developed software (String_analysis.exe) was developed using C# language on Eclipse Java IDE for web developers, Luna Service Release 1 (4.4.1). Voxel information for the VK-phantom, including ID number and *x*, *y* and *z* coordinates, is presented in a row; consequently, the number of rows with identical ID numbers represents the voxel number of a structure (Fig. 2c). After the VK-phantom male and female were opened on String_analysis.exe, the number of rows with identical ID numbers in the phantom was written in the window (Fig. 2d).

Structures of the VK-phantoms were rearranged according to the structure list in Virtual Population. The voxel number of the rearranged structures in the VK-phantoms was multiplied by the structure density (g/mm^3) in Virtual Population [1, 4, 5, 12] to measure the weight of each structure (Tables 2 and 3). However, the densities of some rearranged structures did not follow those of Virtual Population (marked with superscripts 'a' and 'b' in Tables 2 and 3) because the densities reported in Virtual Population were not accurate. For example, in Virtual Population, the density of the cerebellum (1040 kg/m^3) is identical to that of the esophagus and urinary bladder.

RESULTS

From the segmented images based on the male sectioned images of a previous study [17], reduced segmented images were prepared (intervals, 1.0 mm; pixel size, 1.0 mm^2), in which the 583 structures could be sorted by color (Fig. 1b; Table 1). The VK-phantom male was produced based on the reduced segmented images on which the *x*, *y* and *z* coordinates and structure ID numbers were marked (Fig. 2c). In the VK-phantom male, fat was the heaviest structure (8231 g), followed by the lung (3641 g). The lightest structure was the sinoatrial nodal branch (0.01 g). The real weights of the phantom's actual person and the total weight of the phantom were 55 kg [15] and 58 kg, respectively (Table 2).

Similar to the VK-phantom male, the VK-phantom female was produced from the segmented images of the female, with 459 structures (Fig. 1d; Table 1). In the VK-phantom female, fat was the heaviest structure (29 666 g), followed by the skin (1714 g), femur (1684 g) and cranium without the mandible (1084.9 g). The female cranium was heavier than that of the male because the cranium in the phantom was an object, unlike several objects of male cranium (Table 1). The lightest structure was the posterior commissure (0.01 g). The weights of the actual woman and total weight of the phantom were 52 kg [16] and 55 kg, respectively (Table 3).

All structures in the VK-phantom male and female were rearranged according to Virtual Population [1, 11, 20] and sorted mainly by tissue features. In the rearranged VK-phantom male, the muscles (22 780 g) and bones (13 317 g) were heavier than fat (8231 g) in the VK-phantom with 583 structures. In the case of the female, fat was the heaviest structure. Consequently, the VK-phantom female was obese. In both the male and female VK-phantoms, the eye (cornea) was the lightest structure (Table 4).

Furthermore, the rearranged VK-phantoms were compared with the High-Definition Reference Korean Man (HDRK), Virtual Family and ICRP phantoms [1, 4, 5]. The weights of most structures in the four phantoms were similar. However, a few structures (skin, blood, fat and spleen) were very different. In particular, the skins of VK-phantom male and HDRK man were almost twice the weight, although the source images of the VK-phantom male and HDRK man were identical [15]. In the case of the spleen, the VK-phantom's actual person had splenomegaly from leukemia. Therefore, the VK-phantom male's spleen was very heavy (1110 g) compared with that of other phantoms, but the HDRK man's spleen was light (177 g), even though the source images of the two

Table 2. A listing of 583 body structures of the VK-phantom male, and the mass of each structure according to material densities in Virtual Population (2017)

Structures	Number of voxels (A)	Structures in Virtual Population	Substitution structures from Virtual Population	Density [kg/m^3] (B)	Weight (g) (A X B X 0.000001)
Abductor digiti minimi m. (right)	17213	Muscle		1090	18.76
Abductor digiti minimi m. (left)	13969	Muscle		1090	15.23
Abductor hallucis m.	35928	Muscle		1090	39.16
Abductor pollicis brevis m.	13866	Muscle		1090	15.11
Abductor pollicis longus m.	45197	Muscle		1090	49.26
Accessory hemi-azygos v.	1338	Blood		1050	1.40
Acetabular labrum	577	Tendon/Ligament		1142	0.66
Adductor brevis m.	182623	Muscle		1090	199.06
Adductor hallucis m. oblique head	24135	Muscle		1090	26.31
Adductor hallucis m. transverse head	3181	Muscle		1090	3.47
Adductor longus m.	269631	Muscle		1090	293.90
Adductor magnus m.	683101	Muscle		1090	744.58
Adductor pollicis m.	6724	Muscle		1090	7.33
Adenohypophysis	604	Hypophysis		1053	0.64
Air	0	Air		1	0.00
Amygdaloid nucleus	415	Brain (gray matter)		1045	0.43
Anal canal	879	Large intestine		1088	0.96
Anconeus m.	2748	Muscle		1090	3.00
Anterior basal segmental bronchus	589	Bronchi		1102	0.65
Anterior cruciate ligament	798	Tendon/Ligament		1142	0.91
Anterior interventricular branch	981	Blood		1050	1.03
Anterior longitudinal ligament	9646	Tendon/Ligament		1142	11.02
Anterior ramus of fifth lumbar n.	2758	Nerve		1075	2.96
Anterior ramus of first lumbar n.	165	Nerve		1075	0.18
Anterior ramus of first sacral n.	2713	Nerve		1075	2.92
Anterior ramus of fourth lumbar n.	906	Nerve		1075	0.97
Anterior ramus of second lumbar n.	311	Nerve		1075	0.33
Anterior ramus of second sacral n.	2277	Nerve		1075	2.45
Anterior ramus of third lumbar n.	507	Nerve		1075	0.55
Anterior ramus of third sacral n.	642	Nerve		1075	0.69
Anterior rectus capitis m.	1670	Muscle		1090	1.82

Continued

Table 2. Continued

Structures	Number of voxels (A)	Structures in Virtual Population	Substitution structures from Virtual Population	Density [kg/m^3] (B)	Weight (g) (A X B X 0.000001)
Anterior root of fifth lumbar n.	235	Nerve		1075	0.25
Anterior root of first lumbar n.	52	Nerve		1075	0.06
Anterior root of first sacral n.	585	Nerve		1075	0.63
Anterior root of fourth lumbar n.	295	Nerve		1075	0.32
Anterior root of second lumbar n.	48	Nerve		1075	0.05
Anterior root of second sacral n.	464	Nerve		1075	0.50
Anterior root of third lumbar n.	105	Nerve		1075	0.11
Anterior root of third sacral n.	100	Nerve		1075	0.11
Anterior scalenus m.	15727	Muscle		1090	17.14
Anterior segmental bronchus	5526	Bronchi		1102	6.09
Anterior serratus m.	349220	Muscle		1090	380.65
Anterior tibial a.	371	Blood		1050	0.39
Anterior tibialis m.	236332	Muscle		1090	257.60
Aortic valve	847	Cartilage		1100	0.93
Apical segmental bronchus	546	Bronchi		1102	0.60
Apicoposterior segmental bronchus	936	Bronchi		1102	1.03
Appendix	22725	Large intestine		1088	24.72
Arch of aorta	13349	Blood		1050	14.02
Articularis genus m.	2605	Muscle		1090	2.84
Ascending aorta	19325	Blood		1050	20.29
Ascending colon	46238	Large intestine		1088	50.31
Atrioventricular nodal branch	37	Blood		1050	0.04
Auditory tube	66	Cartilage		1100	0.07
Axillary a.	2542	Blood		1050	2.67
Axillary v.	12062	Blood		1050	12.67
Azygos v.	6052	Blood		1050	6.35
Basilar a.	80	Blood		1050	0.08
Basilic v.	1891	Blood		1050	1.99
Biceps brachii m.	191270	Muscle		1090	208.48
Biceps femoris m.	385341	Muscle		1090	420.02
Brachial a.	3369	Blood		1050	3.54

Continued

Table 2. Continued

Structures	Number of voxels (A)	Structures in Virtual Population	Substitution structures from Virtual Population	Density [kg/m^3] (B)	Weight (g) (A X B X 0.000001)
Brachial plexus	3267	Nerve		1075	3.51
Brachial v.	14874	Blood		1050	15.62
Brachialis m.	232229	Muscle		1090	253.13
Brachiocephalic trunk	4631	Blood		1050	4.86
Brachiocephalic vein	13457	Blood		1050	14.13
Brachioradialis m.	98728	Muscle		1090	107.61
Brain (Lateral ventricle)	9984	Cerebrospinal fluid		1007	10.05
Brainstem	30016	Brain		1046	31.40
Buccinator m.	11795	Muscle		1090	12.86
Bulbospongiosus m.	5716	Muscle		1090	6.23
Calcaneum	129770	Bone (cortical)		1908	247.60
Capitate	8381	Bone (cortical)		1908	15.99
Caudate nucleus	14997	Brain (gray matter)		1045	15.67
Cecum	42833	Large intestine		1088	46.60
Celiac trunk	323	Blood		1050	0.34
Cephalic v.	6529	Blood		1050	6.86
Cerebellum[a]	167429	Cerebellum	Brain	1046	175.13
Cervical vertebra (fifth)	15907	Vertebrae		1908	30.35
Cervical vertebra (first)	24574	Vertebrae		1908	46.89
Cervical vertebra (fourth)	15993	Vertebrae		1908	30.51
Cervical vertebra (second)	21579	Vertebrae		1908	41.17
Cervical vertebra (seventh)	21910	Vertebrae		1908	41.80
Cervical vertebra (sixth)	16945	Vertebrae		1908	32.33
Cervical vertebra (third)	16249	Vertebrae		1908	31.00
Circumflex branch	391	Blood		1050	0.41
Claustrum	2879	Brain (gray matter)		1045	3.01
Clavicle	70883	Bone (cortical)		1908	135.24
Coccygeus m.	4182	Muscle		1090	4.56
Coccyx	6351	Bone (cortical)		1908	12.12
Common bile duct[b]	1247		Bile	928	1.16
Common carotid a.	7529	Blood		1050	7.91

Continued

Table 2. Continued

Structures	Number of voxels (A)	Structures in Virtual Population	Substitution structures from Virtual Population	Density [kg/m^3] (B)	Weight (g) (A X B X 0.000001)
Common fibular n.	2436	Nerve		1075	2.62
Common hepatic a.	186	Blood		1050	0.20
Common hepatic duct[b]	1227		Urinary bladder wall	1086	1.33
Common iliac a.	2257	Blood		1050	2.37
Common iliac v.	3047	Blood		1050	3.20
Confluence of sinuses	1069	Blood		1050	1.12
Constrictor m.	17658	Muscle		1090	19.25
Coracobrachialis m.	31862	Muscle		1090	34.73
Coracobrachialis m.	30152	Muscle		1090	32.87
Coronary sinus	3877	Blood		1050	4.07
Corpus cavernosa penis[b]	8292		Blood	1050	8.71
Corpus spongiosum penis[b]	7267		Blood	1050	7.63
Cranium without mandible	97031	Skull cortical		1908	185.14
Cricothyroid m.	1629	Muscle		1090	1.78
Crista galli	274	Skull cortical		1908	0.52
Cuboid	26192	Bone (cortical)		1908	49.97
Cystic a.	18	Blood		1050	0.02
Cystic duct[b]	2180		Bile	928	2.37
Deep brachial a.	429	Blood		1050	0.45
Deep femoral a.	1074	Blood		1050	1.13
Deep fibular n.	1300	Nerve		1075	1.40
Deep transverse perineal m.	3895	Muscle		1090	4.25
Deltoid m.	585531	Muscle		1090	638.23
Descending aorta	56011	Blood		1050	58.81
Descending colon	128518	Large intestine		1088	139.83
Diaphragm	305421	Diaphragm		1090	332.91
Digastric m.	13708	Muscle		1090	14.94
Distal phalanx (fifth)	1009	Bone (cortical)		1908	1.93
Distal phalanx (fifth)	777	Bone (cortical)		1908	1.48
Distal phalanx (first)	4406	Bone (cortical)		1908	8.41
Distal phalanx (first)	4051	Bone (cortical)		1908	7.73

Continued

Table 2. Continued

Structures	Number of voxels (A)	Structures in Virtual Population	Substitution structures from Virtual Population	Density [kg/m^3] (B)	Weight (g) (A X B X 0.000001)
Distal phalanx (fourth)	1388	Bone (cortical)		1908	2.65
Distal phalanx (fourth)	1055	Bone (cortical)		1908	2.01
Distal phalanx (second)	1578	Bone (cortical)		1908	3.01
Distal phalanx (second)	846	Bone (cortical)		1908	1.61
Distal phalanx (third)	1631	Bone (cortical)		1908	3.11
Distal phalanx (third)	835	Bone (cortical)		1908	1.59
Dorsal interossei m.	46077	Muscle		1090	50.22
Ductus deferens[a]	2703	Ductus deferens	Urinary bladder wall	1086	2.94
Duodenum[a]	12398	Small intestine	Urinary bladder wall	1086	13.46
Ejaculatory duct[b]	19		Urinary bladder wall	1086	0.02
Epididymis	9979	Epididymis		1082	10.80
Erector spinae m.	260222	Muscle		1090	283.64
Esophagus (luminal)	6418	Esophagus lumen		1	0.01
Ethmoid bone	64932	Skull cortical		1908	123.89
Ethmoidal cells	2296	Air		1	0.00
Extensor carpi radialis brevis m.	31153	Muscle		1090	33.96
Extensor carpi radialis longus m.	95726	Muscle		1090	104.34
Extensor carpi ulnaris m.	66797	Muscle		1090	72.81
Extensor digiti minimi m.	15904	Muscle		1090	17.34
Extensor digitorum brevis m.	22753	Muscle		1090	24.80
Extensor digitorum longus m.	121812	Muscle		1090	132.78
Extensor digitorum m.	78107	Muscle		1090	85.14
Extensor hallucis longus m.	48025	Muscle		1090	52.35
Extensor indicis m.	5921	Muscle		1090	6.45
Extensor indicis m.	5810	Muscle		1090	6.33
Extensor pollicis brevis m.	1441	Muscle		1090	1.57
Extensor pollicis longus m.	14067	Muscle		1090	15.33
External acoustic meatus	2327	Bone (cortical)		1908	4.44
External anal sphincter m.	10627	Muscle		1090	11.58
External carotid a.	549	Blood		1050	0.58
External iliac a.	2064	Blood		1050	2.17

Continued

Table 2. Continued

Structures	Number of voxels (A)	Structures in Virtual Population	Substitution structures from Virtual Population	Density [kg/m^3] (B)	Weight (g) (A X B X 0.000001)
External iliac v.	6088	Blood		1050	6.39
External oblique abdominal m.	372614	Muscle		1090	406.15
External urethral sphincter m.	485	Muscle		1090	0.53
Eye (choroid)	1318	Blood		1050	1.38
Eye (cornea)	16	Eye (cornea)		1051	0.02
Eye (lens)	512	Eye (lens)		1076	0.55
Eye (sclera)	1330	Eye (sclera)		1032	1.37
Eye (vitreous humor)	15293	Eye (vitreous humor)		1005	15.37
Fat	8986675.5	Fat		911	8186.86
Femoral a.	3634	Blood		1050	3.82
Femoral n.	5419	Nerve		1075	5.83
Femoral v.	12552	Blood		1050	13.18
Femur	967336	Bone (cortical)		1908	1845.68
Fibula	104947	Bone (cortical)		1908	200.24
Fibular collateral ligament	305	Tendon/Ligament		1142	0.35
Fibularis brevis m.	52954	Muscle		1090	57.72
Fibularis longus m.	129684	Muscle		1090	141.36
Flexor carpi radialis m.	56974	Muscle		1090	62.10
Flexor carpi ulnaris m.	63893	Muscle		1090	69.64
Flexor digiti minimi brevis m.	11457	Muscle		1090	12.49
Flexor digiti minimi brevis m.	11248	Muscle		1090	12.26
Flexor digitorum brevis m.	30426	Muscle		1090	33.16
Flexor digitorum longus m.	62679	Muscle		1090	68.32
Flexor digitorum profundus m.	207929	Muscle		1090	226.64
Flexor digitorum superficialis m.	151250	Muscle		1090	164.86
Flexor hallucis brevis m.	10032	Muscle		1090	10.93
Flexor hallucis longus m.	155955	Muscle		1090	169.99
Flexor pollicis brevis m.	23662	Muscle		1090	25.79
Flexor pollicis longus m.	45785	Muscle		1090	49.91
Fornix	1296	Brain (white matter)		1041	1.35
Frontal bone	124074	Skull cortical		1908	236.73

Continued

Table 2. Continued

Structures	Number of voxels (A)	Structures in Virtual Population	Substitution structures from Virtual Population	Density [kg/m^3] (B)	Weight (g) (A X B X 0.000001)
Frontal lobe	643551	Brain		1046	673.15
Frontal sinus	577	Air		1	0.00
Gallbladder	120901	Gallbladder		1071	129.48
Gastrocnemius m.	676601	Muscle		1090	737.50
Gastroduodenal a.	151	Blood		1050	0.16
Genioglossus m.	4725	Muscle		1090	5.15
Geniohyoid m.	14376	Muscle		1090	15.67
Globus pallidus	5258	Brain (gray matter)		1045	5.49
Gluteus maximus m.	1202406	Muscle		1090	1310.62
Gluteus medius m.	566187	Muscle		1090	617.14
Gluteus minimus m.	228904	Muscle		1090	249.51
Gracilis m.	137861	Muscle		1090	150.27
Great cardiac v.	1340	Blood		1050	1.41
Great saphenous v.	4193	Blood		1050	4.40
Hamate	6827	Bone (cortical)		1908	13.03
Heart	471330	Heart muscle		1081	509.51
Hemi-azygos v.	1511	Blood		1050	1.59
Hepatopancreatic ampulla[b]	74		Urinary bladder wall	1086	0.08
Hip bone	671402	Bone (cortical)		1908	1281.04
Humerus	200323	Bone (cortical)		1908	382.22
Humerus	178333	Bone (cortical)		1908	340.26
Hyoglossus m.	4894	Muscle		1090	5.33
Iliacus m.	107410	Muscle		1090	117.08
Iliocostalis lumborum m.	28812	Muscle		1090	31.41
Iliocostalis m.	301899	Muscle		1090	329.07
Iliopsoas m.	228082	Muscle		1090	248.61
Inferior epigastric a.	17	Blood		1050	0.02
Inferior gemellus m.	15816	Muscle		1090	17.24
Inferior gluteal a.	269	Blood		1050	0.28
Inferior gluteal n.	506	Nerve		1075	0.54
Inferior lingular segmental bronchus	1034	Bronchi		1102	1.14

Continued

Table 2. Continued

Structures	Number of voxels (A)	Structures in Virtual Population	Substitution structures from Virtual Population	Density [kg/m^3] (B)	Weight (g) (A X B X 0.000001)
Inferior lobar bronchus	2976	Bronchi		1102	3.28
Inferior mesenteric a.	379	Blood		1050	0.40
Inferior mesenteric v.	908	Blood		1050	0.95
Inferior oblique m.	817	Muscle		1090	0.89
Inferior obliquus capitis m.	20476	Muscle		1090	22.32
Inferior pulmonary v.	11292	Blood		1050	11.86
Inferior rectus m.	1588	Muscle		1090	1.73
Inferior sagittal sinus	573	Blood		1050	0.60
Inferior vena cava	69434	Blood		1050	72.91
Inferior vesical a.	70	Blood		1050	0.07
Infraspinatus m.	230155	Muscle		1090	250.87
Intercostal m.	1153097	Muscle		1090	1256.88
Intermediate cuneiform	9622	Bone (cortical)		1908	18.36
Intermediate hepatic v.	5775	Blood		1050	6.06
Intermediate part of urethra[a]	55	Ureter/Urethra	Urinary bladder wall	1086	0.06
Internal carotid a.	3123	Blood		1050	3.28
Internal iliac a.	660	Blood		1050	0.69
Internal iliac v.	116	Blood		1050	0.12
Internal jugular v.	4627	Blood		1050	4.86
Internal oblique abdominal m.	176340	Muscle		1090	192.21
Internal pudendal a.	127	Blood		1050	0.13
Interspinous ligament (L I–L II)	366	Tendon/Ligament		1142	0.42
Interspinous ligament (L II–L III)	322	Tendon/Ligament		1142	0.37
Interspinous ligament (L III–L IV)	729	Tendon/Ligament		1142	0.83
Interspinous ligament (L IV–L V)	624	Tendon/Ligament		1142	0.71
Interspinous ligament (L V–sacrum)	1147	Tendon/Ligament		1142	1.31
Intervertebral disc (C II–C III)	1475	Intervertebral disc		1100	1.62
Intervertebral disc (C III–C IV)	1457	Intervertebral disc		1100	1.60
Intervertebral disc (C IV–C V)	1400	Intervertebral disc		1100	1.54
Intervertebral disc (C V–C VI)	1915	Intervertebral disc		1100	2.11
Intervertebral disc (C VI–C VII)	2464	Intervertebral disc		1100	2.71

Continued

Table 2. Continued

Structures	Number of voxels (A)	Structures in Virtual Population	Substitution structures from Virtual Population	Density [kg/m^3] (B)	Weight (g) (A X B X 0.000001)
Intervertebral disc (C VII–T I)	2635	Intervertebral disc		1100	2.90
Intervertebral disc (L I–L II)	12552	Intervertebral disc		1100	13.81
Intervertebral disc (L II–L III)	17279	Intervertebral disc		1100	19.01
Intervertebral disc (L III–L IV)	18428	Intervertebral disc		1100	20.27
Intervertebral disc (L IV–L V)	21523	Intervertebral disc		1100	23.68
Intervertebral disc (L V–Sacrum)	16300	Intervertebral disc		1100	17.93
Intervertebral disc (T I–T II)	3046	Intervertebral disc		1100	3.35
Intervertebral disc (T II–T III)	2970	Intervertebral disc		1100	3.27
Intervertebral disc (T III–T IV)	3235	Intervertebral disc		1100	3.56
Intervertebral disc (T IV–T V)	3414	Intervertebral disc		1100	3.76
Intervertebral disc (T IX–T X)	6052	Intervertebral disc		1100	6.66
Intervertebral disc (T V–T VI)	3606	Intervertebral disc		1100	3.97
Intervertebral disc (T VI–T VII)	3634	Intervertebral disc		1100	4.00
Intervertebral disc (T VII–T VIII)	4931	Intervertebral disc		1100	5.42
Intervertebral disc (T VIII–T IX)	5417	Intervertebral disc		1100	5.96
Intervertebral disc (T X–T XI)	5865	Intervertebral disc		1100	6.45
Intervertebral disc (T XI–T XII)	8317	Intervertebral disc		1100	9.15
Intervertebral disc (T XII–L I)	10008	Intervertebral disc		1100	11.01
Ischiocavernosus m.	7463	Muscle		1090	8.13
Jejunum and ileum[a]	634989	Small intestine	Urinary bladder wall	1086	689.60
Kidney	405956	Kidney		1066	432.75
Lacrimal bone	1508	Bone (cortical)		1908	2.88
Larynx	2492	Cartilage		1100	2.74
Lateral basal segmental bronchus	463	Bronchi		1102	0.51
Lateral crico-arytenoid m.	2771	Muscle		1090	3.02
Lateral cuneiform	11119	Bone (cortical)		1908	21.22
Lateral mandibular incisor tooth	641	Tooth		2180	1.40
Lateral maxillary incisor tooth	744	Tooth		2180	1.62
Lateral meniscus	586	Meniscus		1100	0.64
Lateral pterygoid m.	21982	Muscle		1090	23.96
Lateral rectus m.	1868	Muscle		1090	2.04

Continued

Table 2. Continued

Structures	Number of voxels (A)	Structures in Virtual Population	Substitution structures from Virtual Population	Density [kg/m^3] (B)	Weight (g) (A X B X 0.000001)
Lateral segmental bronchus	592	Bronchi		1102	0.65
Latissimus dorsi m.	489955	Muscle		1090	534.05
Left atrium	60060	Heart muscle		1081	64.92
Left coronary a.	164	Blood		1050	0.17
Left gastric a.	19	Blood		1050	0.02
Left hepatic duct[b]	1042		Urinary bladder wall	1086	1.13
Left hepatic v.	463	Blood		1050	0.49
Left marginal a.	272	Blood		1050	0.29
Left ventricle	29555	Heart muscle		1081	31.95
Levator ani m.	28066	Muscle		1090	30.59
Levator palpebrae superioris m.	1033	Muscle		1090	1.13
Levator scapulae m.	70957	Muscle		1090	77.34
Levator veli palatini	3996	Muscle		1090	4.36
Ligament of head of femur	3069	Tendon/Ligament		1142	3.50
Ligamentum flavum (L I–L II)	1278	Tendon/Ligament		1142	1.46
Ligamentum flavum (L II–L III)	2177	Tendon/Ligament		1142	2.49
Ligamentum flavum (L III–L IV)	2432	Tendon/Ligament		1142	2.78
Ligamentum flavum (L IV–L V)	2544	Tendon/Ligament		1142	2.91
Ligamentum flavum (L V–sacrum)	2094	Tendon/Ligament		1142	2.39
Liver	2025510	Liver		1079	2185.53
lliolumbar a.	50	Blood		1050	0.05
Longissimus capitis m.	11299	Muscle		1090	12.32
Longissimus cervicis m.	108146	Muscle		1090	117.88
Longissimus m.	215670	Muscle		1090	235.08
Longus capitis m.	20392	Muscle		1090	22.23
Longus colli m.	33151	Muscle		1090	36.13
Lumbar vertebra (fifth)	64122	Bone (cortical)		1908	122.34
Lumbar vertebra (first)	57223	Bone (cortical)		1908	109.18
Lumbar vertebra (fourth)	65315	Bone (cortical)		1908	124.62
Lumbar vertebra (second)	59502	Bone (cortical)		1908	113.53
Lumbar vertebra (third)	63579	Bone (cortical)		1908	121.31

Continued

Table 2. Continued

Structures	Number of voxels (A)	Structures in Virtual Population	Substitution structures from Virtual Population	Density [kg/m^3] (B)	Weight (g) (A X B X 0.000001)
Lumbrical m.	4781	Muscle		1090	5.21
Lunate	4263	Bone (cortical)		1908	8.13
Lung	5559526	Lung		394	2190.45
Main bronchus	8404	Bronchi		1102	9.26
Mandible	88747	Mandible		1908	169.33
Mandibular canine tooth	958	Tooth		2180	2.09
Mandibular molar tooth (first)	2504	Tooth		2180	5.46
Mandibular molar tooth (second)	1039	Tooth		2180	2.27
Mandibular premolar tooth (first)	841	Tooth		2180	1.83
Mandibular premolar tooth (second)	1857	Tooth		2180	4.05
Masseter m.	59529	Muscle		1090	64.89
Maxilla	1408	Skull cortical		1908	2.69
Maxillary canine tooth	1224	Tooth		2180	2.67
Maxillary molar tooth (first)	2387	Tooth		2180	5.20
Maxillary molar tooth (second)	2336	Tooth		2180	5.09
Maxillary premolar tooth (first)	894	Tooth		2180	1.95
Maxillary premolar tooth (second)	826	Tooth		2180	1.80
Maxillary sinus	19843	Air		1	0.02
Medial basal segmental bronchus	765	Bronchi		1102	0.84
Medial cuneiform	20732	Bone (cortical)		1908	39.56
Medial mandibular incisor tooth	438	Tooth		2180	0.95
Medial maxillary incisor tooth	998	Tooth		2180	2.18
Medial meniscus	511	Meniscus		1100	0.56
Medial pterygoid m.	22926	Muscle		1090	24.99
Medial rectus m.	1679	Muscle		1090	1.83
Medial segmental bronchus	394	Bronchi		1102	0.43
Median n.	4490	Nerve		1075	4.83
Metacarpal bone (fifth)	9834	Bone (cortical)		1908	18.76
Metacarpal bone (first)	12821	Bone (cortical)		1908	24.46
Metacarpal bone (fourth)	11714	Bone (cortical)		1908	22.35
Metacarpal bone (second)	16559	Bone (cortical)		1908	31.59

Continued

Table 2. Continued

Structures	Number of voxels (A)	Structures in Virtual Population	Substitution structures from Virtual Population	Density [kg/m^3] (B)	Weight (g) (A X B X 0.000001)
Metacarpal bone (third)	14973	Bone (cortical)		1908	28.57
Metacarpal bone (third)	832	Bone (cortical)		1908	1.59
Metatarsal bone (fifth)	20200	Bone (cortical)		1908	38.54
Metatarsal bone (first)	35661	Bone (cortical)		1908	68.04
Metatarsal bone (fourth)	14531	Bone (cortical)		1908	27.73
Metatarsal bone (second)	16989	Bone (cortical)		1908	32.42
Metatarsal bone (third)	14934	Bone (cortical)		1908	28.49
Middle cardiac v.	621	Blood		1050	0.65
Middle lobar bronchus	498	Bronchi		1102	0.55
Middle phalanx (fifth)	1709	Bone (cortical)		1908	3.26
Middle phalanx (fifth)	1618	Bone (cortical)		1908	3.09
Middle phalanx (fourth)	3242	Bone (cortical)		1908	6.19
Middle phalanx (fourth)	1081	Bone (cortical)		1908	2.06
Middle phalanx (second)	2959	Bone (cortical)		1908	5.65
Middle phalanx (second)	2098	Bone (cortical)		1908	4.00
Middle phalanx (third)	3567	Bone (cortical)		1908	6.81
Middle phalanx (third)	1248	Bone (cortical)		1908	2.38
Middle scalenus m.	16175	Muscle		1090	17.63
Mitral valve[b]	1068	Cartilage		1100	1.17
Mylohyoid m.	11805	Muscle		1090	12.87
Nasal bone	1513	Bone (cortical)		1908	2.89
Nasal cavity	24884	Air		1	0.02
Navicular	21746	Bone (cortical)		1908	41.49
Neurohypophysis	165	Hypophysis		1053	0.17
Obturator a.	179	Blood		1050	0.19
Obturator externus m.	100148	Muscle		1090	109.16
Obturator internus m.	104060	Muscle		1090	113.43
Obturator n.	1948	Nerve		1075	2.09
Occipital bone	93619	Skull cortical		1908	178.63
Occipital lobe	188142	Brain		1046	196.80
Occipital sinus	158	Blood		1050	0.17

Continued

Table 2. Continued

Structures	Number of voxels (A)	Structures in Virtual Population	Substitution structures from Virtual Population	Density [kg/m^3] (B)	Weight (g) (A X B X 0.000001)
Omohyoid m.	10326	Muscle		1090	11.26
Opponens digiti minimi m.	7415	Muscle		1090	8.08
Opponens pollicis m.	12861	Muscle		1090	14.02
Optic n.	2102	Nerve		1075	2.26
Palatoglossus m.	465	Muscle		1090	0.51
Palmar interossei m.	12093	Muscle		1090	13.18
Palmaris brevis m.	2255	Muscle		1090	2.46
Palmaris longus m.	29351	Muscle		1090	31.99
Pancreas	113805	pancreas		1087	123.71
Pancreatic duct[b]	114		Urinary bladder wall	1086	0.12
Parietal bone	268496	Skull cortical		1908	512.29
Parietal lobe	307372	Brain		1046	321.51
Parotid gland	47885	Salivary gland		1048	50.18
Patella	23082	Bone (cortical)		1908	44.04
Patella	22560	Bone (cortical)		1908	43.04
Pectineus m.	93609	Muscle		1090	102.03
Pectoralis major m.	478970	Muscle		1090	522.08
Pectoralis minor m.	43616	Muscle		1090	47.54
Pericardial cavity	229330	Cerebrospinal fluid		1007	230.94
Pharynx	1482	Pharynx		1	0.00
Piriformis m.	76195	Muscle		1090	83.05
Pisiform	1916	Bone (cortical)		1908	3.66
Plantar interossei m.	35274	Muscle		1090	38.45
Plantaris m.	18365	Muscle		1090	20.02
Popliteal a.	1070	Blood		1050	1.12
Popliteal v.	1898	Blood		1050	1.99
Popliteus m.	43436	Muscle		1090	47.35
Posterior basal segmental bronchus	4504	Bronchi		1102	4.96
Posterior basal segmental bronchus	262	Bronchi		1102	0.29
Posterior crico-arytenoid m.	910	Muscle		1090	0.99
Posterior cruciate ligament	702	Tendon/Ligament		1142	0.80

Continued

Table 2. Continued

Structures	Number of voxels (A)	Structures in Virtual Population	Substitution structures from Virtual Population	Density [kg/m^3] (B)	Weight (g) (A X B X 0.000001)
Posterior interventricular branch	37	Blood		1050	0.04
Posterior longitudinal ligament	1351	Tendon/Ligament		1142	1.54
Posterior rectus capitis major m.	10500	Muscle		1090	11.45
Posterior rectus capitis minor m.	5169	Muscle		1090	5.63
Posterior root of fifth lumbar n.	1143	Nerve		1075	1.23
Posterior root of first sacral n.	1408	Nerve		1075	1.51
Posterior root of fourth lumbar n.	596	Nerve		1075	0.64
Posterior root of second lumbar n.	172	Nerve		1075	0.18
Posterior root of second sacral n.	825	Nerve		1075	0.89
Posterior root of third lumbar n.	255	Nerve		1075	0.27
Posterior root of third sacral n.	508	Nerve		1075	0.55
Posterior scalenus m.	43678	Muscle		1090	47.61
Posterior segmental bronchus	1104	Bronchi		1102	1.22
Posterior superior serratus m.	16738	Muscle		1090	18.24
Posterior tibial a.	3371	Blood		1050	3.54
Posterior tibialis m.	166872	Muscle		1090	181.89
Preprostatic part of urethra[a]	20	Ureter/Urethra	Urinary bladder wall	1086	0.02
Pronator quadratus m.	26236	Muscle		1090	28.60
Pronator teres m.	47628	Muscle		1090	51.91
Proper hepatic a.	86	Blood		1050	0.09
Prostate[b]	11524	Prostate	Salivary gland	1048	12.08
Prostatic urethra[a]	63	Ureter/Urethra	Urinary bladder wall	1086	0.07
Proximal phalanx (fifth)	5029	Bone (cortical)		1908	9.60
Proximal phalanx (fifth)	1006	Bone (cortical)		1908	1.92
Proximal phalanx (first)	11330	Bone (cortical)		1908	21.62
Proximal phalanx (first)	4962	Bone (cortical)		1908	9.47
Proximal phalanx (fourth)	7967	Bone (cortical)		1908	15.20
Proximal phalanx (fourth)	1696	Bone (cortical)		1908	3.24
Proximal phalanx (second)	8022	Bone (cortical)		1908	15.31
Proximal phalanx (second)	2429	Bone (cortical)		1908	4.63
Proximal phalanx (third)	9243	Bone (cortical)		1908	17.64

Continued

Table 2. Continued

Structures	Number of voxels (A)	Structures in Virtual Population	Substitution structures from Virtual Population	Density [kg/m^3] (B)	Weight (g) (A X B X 0.000001)
Proximal phalanx (third)	1646	Bone (cortical)		1908	3.14
Psoas major m.	334209	Muscle		1090	364.29
Pulmonary a.	55026	Blood		1050	57.78
Pulmonary trunk	3327	Blood		1050	3.49
Pulmonary valve	1411	Cartilage		1100	1.55
Putamen	17360	Brain (gray matter)		1045	18.14
Quadratus femoris m.	51750	Muscle		1090	56.41
Quadratus lumborum m.	143118	Muscle		1090	156.00
Quadratus plantae m.	14728	Muscle		1090	16.05
Radial a.	1651	Blood		1050	1.73
Radial n.	457	Nerve		1075	0.49
Radius	107692	Bone (cortical)		1908	205.48
Rectum	113149	Large intestine		1088	123.11
Rectus abdominis m.	329625	Muscle		1090	359.29
Rectus capitis lateralis m.	2805	Muscle		1090	3.06
Rectus femoris m.	354178	Muscle		1090	386.05
Renal v.	15298	Blood		1050	16.06
Rhomboid major m.	81703	Muscle		1090	89.06
Rhomboid minor m.	8439	Muscle		1090	9.20
Rib (eighth)	99949	Bone (cortical)		1908	190.70
Rib (eleventh)	30168	Bone (cortical)		1908	57.56
Rib (fifth)	83661	Bone (cortical)		1908	159.63
Rib (first)	39267	Bone (cortical)		1908	74.92
Rib (fourth)	72344	Bone (cortical)		1908	138.03
Rib (ninth)	72496	Bone (cortical)		1908	138.32
Rib (second)	45192	Bone (cortical)		1908	86.23
Rib (seventh)	121273	Bone (cortical)		1908	231.39
Rib (sixth)	103318	Bone (cortical)		1908	197.13
Rib (tenth)	50557	Bone (cortical)		1908	96.46
Rib (third)	55217	Bone (cortical)		1908	105.35
Rib (twelfth)	14901	Bone (cortical)		1908	28.43

Continued

Table 2. Continued

Structures	Number of voxels (A)	Structures in Virtual Population	Substitution structures from Virtual Population	Density [kg/m^3] (B)	Weight (g) (A X B X 0.000001)
Right atrium	105829	Heart lumen		1050	111.12
Right coronary a.	431	Blood		1050	0.45
Right hepatic duct[b]	370		Urinary bladder wall	1086	0.40
Right hepatic v.	7202	Blood		1050	7.56
Right ventricle	91189	Heart lumen		1050	95.75
Sacrospinous ligament	1450	Tendon/Ligament		1142	1.66
Sacrotuberous ligament	7126	Tendon/Ligament		1142	8.14
Sacrum	206057	Bone (cortical)		1908	393.16
Sartorius m.	232275	Muscle		1090	253.18
Scaphoid	6499	Bone (cortical)		1908	12.40
Scapula	187018	Bone (cortical)		1908	356.83
Sciatic n.	33686	Nerve		1075	36.21
Semimembranosus m.	285635	Muscle		1090	311.34
Seminal vesicle[a]	3882	Seminal vesicle	Salivary gland	1048	4.07
Semispinalis capitis m.	125220	Muscle		1090	136.49
Semispinalis cervicis m.	103928	Muscle		1090	113.28
Semitendinosus m.	234665	Muscle		1090	255.78
Sigmoid colon	81288	Large intestine		1088	88.44
Sigmoid sinus	5950	Blood		1050	6.25
Sinu-atrial nodal branch	6	Blood		1050	0.01
Skin	1610895	Skin		1109	1786.48
Small cardiac v.	157	Blood		1050	0.16
Small saphenous v.	134	Blood		1050	0.14
Soft palate	1664	Muscle		1090	1.81
Soleus m.	624893	Muscle		1090	681.13
Sphenoidal sinus	5326	Air		1	0.01
Spinal cord	39578	Spinal cord		1075	42.55
Spleen	1019875	Spleen		1089	1110.64
Splenic a.	428	Blood		1050	0.45
Splenic v.	4773	Blood		1050	5.01
Splenius capitis m.	74175	Muscle		1090	80.85

Continued

Table 2. Continued

Structures	Number of voxels (A)	Structures in Virtual Population	Substitution structures from Virtual Population	Density [kg/m^3] (B)	Weight (g) (A X B X 0.000001)
Spongy urethra[a]	197	Ureter/Urethra	Urinary bladder wall	1086	0.21
Sternocleidomastoid m.	101243	Muscle		1090	110.35
Sternohyoid m.	19414	Muscle		1090	21.16
Sternothyroid m.	10821	Muscle		1090	11.79
Sternum	72818	Bone (cortical)		1908	138.94
Stomach (luminal)	197999	Stomach lumen		1045	206.91
Straight sinus	656	Blood		1050	0.69
Styloglossus m.	2085	Muscle		1090	2.27
Stylohyoid m.	2806	Muscle		1090	3.06
Stylopharyngeus m.	2298	Muscle		1090	2.50
Subclavian a.	3585	Blood		1050	3.76
Subclavian v.	25168	Blood		1050	26.43
Subclavius m.	11287	Muscle		1090	12.30
Sublingual gland	6020	Salivary gland		1048	6.31
Submandibular gland	20356	Salivary gland		1048	21.33
Subscapularis m.	305109	Muscle		1090	332.57
Superficial fibular n.	1176	Nerve		1075	1.26
Superficial transverse perineal m.	1471	Muscle		1090	1.60
Superior gemellus m.	10618	Muscle		1090	11.57
Superior gluteal a.	317	Blood		1050	0.33
Superior gluteal n.	347	Nerve		1075	0.37
Superior lingular segmental bronchus	1022	Bronchi		1102	1.13
Superior lobar bronchus	1878	Bronchi		1102	2.07
Superior mesenteric a.	1957	Blood		1050	2.05
Superior mesenteric v.	6547	Blood		1050	6.87
Superior oblique m.	696	Muscle		1090	0.76
Superior obliquus capitis m.	10069	Muscle		1090	10.98
Superior pulmonary v.	15171	Blood		1050	15.93
Superior rectus m.	935	Muscle		1090	1.02
Superior sagittal sinus	9145	Blood		1050	9.60
Superior segmental bronchus	1405	Bronchi		1102	1.55

Continued

Table 2. Continued

Structures	Number of voxels (A)	Structures in Virtual Population	Substitution structures from Virtual Population	Density [kg/m^3] (B)	Weight (g) (A X B X 0.000001)
Superior vena cava	9136	Blood		1050	9.59
Supinator m.	43718	Muscle		1090	47.65
Supraspinatus m.	126043	Muscle		1090	137.39
Supraspinous ligament	1803	Tendon/Ligament		1142	2.06
Talus	70679	Bone (cortical)		1908	134.86
Temporal bone	146314	Skull cortical		1908	279.17
Temporal lobe	393665	Brain		1046	411.77
Temporal m.	108724	Muscle		1090	118.51
Tensor fasciae latae m.	105107	Muscle		1090	114.57
Tensor veli palatini	1546	Muscle		1090	1.69
Teres major m.	156281	Muscle		1090	170.35
Teres minor m.	63583	Muscle		1090	69.31
Testis	22741	Testis		1082	24.61
Thalamus[a]	23275	Thalamus	Brain	1046	24.35
Thoracic vertebra (eighth)	32639	Vertebrae		1908	62.28
Thoracic vertebra (eleventh)	43801	Vertebrae		1908	83.57
Thoracic vertebra (fifth)	28291	Vertebrae		1908	53.98
Thoracic vertebra (first)	28953	Vertebrae		1908	55.24
Thoracic vertebra (fourth)	26982	Vertebrae		1908	51.48
Thoracic vertebra (ninth)	34628	Vertebrae		1908	66.07
Thoracic vertebra (second)	29413	Vertebrae		1908	56.12
Thoracic vertebra (seventh)	31619	Vertebrae		1908	60.33
Thoracic vertebra (sixth)	30912	Vertebrae		1908	58.98
Thoracic vertebra (tenth)	38573	Vertebrae		1908	73.60
Thoracic vertebra (third)	26894	Vertebrae		1908	51.31
Thoracic vertebra (twelfth)	49603	Vertebrae		1908	94.64
Thyrohyoid m.	3461	Muscle		1090	3.77
Thyroid gland[a]	17563	Thyroid gland	Salivary gland	1048	18.41
Tibia	623990	Bone (cortical)		1908	1190.57
Tibial collateral ligament	870	Tendon/Ligament		1142	0.99
Tibial n.	19	Nerve		1075	0.02

Continued

Table 2. Continued

Structures	Number of voxels (A)	Structures in Virtual Population	Substitution structures from Virtual Population	Density [kg/m^3] (B)	Weight (g) (A X B X 0.000001)
Tongue	45432	Tongue		1090	49.52
Trachea[a]	25286	Trachea	Bronchi	1102	27.87
Transverse acetabular ligament	1406	Tendon/Ligament		1142	1.61
Transverse colon	252123	Large intestine		1088	274.31
Transverse sinus	5745	Blood		1050	6.03
Transversospinales m.	423987	Muscle		1090	462.15
Transversus abdominis m.	154582	Muscle		1090	168.49
Trapezium	4933	Bone (cortical)		1908	9.41
Trapezius m.	320406	Muscle		1090	349.24
Trapezoid	3778	Bone (cortical)		1908	7.21
Triceps brachii m.	674910	Muscle		1090	735.65
Tricuspid valve[b]	1151	Cartilage		1100	1.27
Triquetrum	3488	Bone (cortical)		1908	6.66
Tympanic cavity	452	Air		1	0.00
Ulna	123461	Bone (cortical)		1908	235.56
Ulnar a.	864	Blood		1050	0.91
Ulnar n.	1464	Nerve		1075	1.57
Ureter[a]	2734	Ureter/Urethra	Urinary bladder wall	1086	2.97
Urinary bladder (luminal)	3742	Urine		1024	3.83
Urinary bladder (mural)	41575	Urinary bladder wall		1086	45.15
Vastus intermedius m.	559200	Muscle		1090	609.53
Vastus lateralis m.	944874	Muscle		1090	1029.91
Vastus medialis m.	541804	Muscle		1090	590.57
Vertebral a.	786	Blood		1050	0.83
Zygomatic bone	31918	Bone (cortical)		1908	60.90
		Total number		583	
		Total weight		58 kg	

a. = artery; m. = muscle; n. = nerve; v. = vein.
[a]Change in the structure of the optimal density on list of Virtual Population (2017) because density of structures in Virtual Population was incorrect.
[b]Assigned to the most similar structures in the Virtual Population (2017) because there was no structure on the list.

phantoms were also identical [15]. Regarding the total weight, the VK-phantom male and HDRK man were 58 kg and 68 kg, respectively (the actual man's weight was 55 kg). The source images of the VK-phantom female and HDRK woman were identical, and the VK-phantom and HDRK woman had similar weights, 55 kg and 52 kg, respectively (the actual woman's weight was 52 kg) (Table 4).

Table 3. Listing of 459 structures of whole body in the VK-phantom female and the weight of each structure according to material density of Virtual Population (2017)

Structures	Number of voxel (A)	Structures of Virtual Population	[a]Substitution structures from Virtual Population	Density [kg/m^3] (B)	Weight (g) (A X B X 0.000001)
Abdominal aorta	12147	Blood		1050	12.75
Abductor digiti minimi m.	636	Muscle		1090	0.69
Abductor hallucis m	30659	Muscle		1090	33.42
Acromioclavicular ligament	1222	Tendon/Ligament		1142	1.40
Adductor longus m.	121655	Muscle		1090	132.60
Adductor magnus m.	500596	Muscle		1090	545.65
Adrenal gland	12999	Adrenal gland		1028	13.36
Air	0	Air		1	0.00
Anal canal	50	Large intestine		1088	0.05
Angular gyrus	46893	Brain (gray matter)		1045	49.00
Anterior commissure	8	Commissura anterior		1041	0.01
Anterior cruciate ligament	2291	Tendon/ligament		1142	2.62
Anterior rectus capitis m.	748	Muscle		1090	0.82
Anterior scalenus m.	10089	Muscle		1090	11.00
Anterior serratus m.	52069	Muscle		1090	56.76
Arch of aorta	8940	Blood		1050	9.39
Aryepiglottis m.	126	Muscle		1090	0.14
Arytenoid cartilage	371	Cartilage		1100	0.41
Ascending aorta	11789	Blood		1050	12.38
Ascending colon	157441	Large intestine		1088	171.30
Basal nucleus	20849	Brain (gray matter)		1045	21.79
Biceps brachii m.	107529	Muscle		1090	117.21
Biceps brachii(long head)	689	Muscle		1090	0.75
Biceps femoris long head m.	146219	Muscle		1090	159.38
Biceps femoris short head m.	65377	Muscle		1090	71.26
Brachialis m.	142515	Muscle		1090	155.34
Brachiocephalic trunk	2498	Blood		1050	2.62
Brachiocephalic v.	7294	Blood		1050	7.66
Brachioradialis m.	5736	Muscle		1090	6.25
Brain (ventricle)	5654	Cerebrospinal fluid		1007	5.69
Brain (white matter)	87493	Brain (white matter)		1041	91.08

Continued

Table 3. Continued

Structures	Number of voxel (A)	Structures of Virtual Population	[a]Substitution structures from Virtual Population	Density [kg/m^3] (B)	Weight (g) (A X B X 0.000001)
Breast	242734	Breast fat		911	221.13
Buccinator m.	6894	Muscle		1090	7.51
Calcaneum	102910	Bone (cortical)		1908	196.35
Capitate	4616	Bone (cortical)		1908	8.81
Cecum	53664	Large intestine		1088	58.39
Celiac trunk	315	Blood		1050	0.33
Cerebellum	112294	Cerebellum		1046	117.46
Cerebrum	82935	Brain		1046	86.75
Cervical vertebra (fifth)	7890	Vertebrae		1908	15.05
Cervical vertebra (first)	10158	Vertebrae		1908	19.38
Cervical vertebra (fourth)	7566	Vertebrae		1908	14.44
Cervical vertebra (second)	12201	Vertebrae		1908	23.28
Cervical vertebra (seventh)	10168	Vertebrae		1908	19.40
Cervical vertebra (sixth)	9393	Vertebrae		1908	17.92
Cervical vertebra (third)	7519	Vertebrae		1908	14.35
Cingulate gyrus	23808	Brain (gray matter)		1045	24.88
Clavicle	38424	Bone (cortical)		1908	73.31
Coccyx	1624	Bone (cortical)		1908	3.10
Common bile duct	2276	Bile		928	2.11
Common carotid a.	6442	Blood		1050	6.76
Common fibular n.	8988	Nerve		1075	9.66
Common hepatic a.	168	Blood		1050	0.18
Common iliac a.	2056	Blood		1050	2.16
Coraco-acromial ligament	619	Tendon/Ligament		1142	0.71
Coracobrachialis m.	15056	Muscle		1090	16.41
Coracoclavicular ligamnet	2253	Tendon/Ligament		1142	2.57
Coracohumeral ligament	363	Tendon/Ligament		1142	0.41
Corniculate cartilage	38	Cartilage		1100	0.04
Coronary sinus	1098	Blood		1050	1.15
Costal cartilage	85302	Cartilage		1100	93.83
Cranium without mandible	545166	Skull cortical		1908	1040.18

Continued

Table 3. Continued

Structures	Number of voxel (A)	Structures of Virtual Population	[a]Substitution structures from Virtual Population	Density [kg/m^3] (B)	Weight (g) (A X B X 0.000001)
Cricoid cartilage	2270	Cartilage		1100	2.50
Cricothyroid ligament	95	Tendon/Ligament		1142	0.11
Cricothyroid m.	1112	Muscle		1090	1.21
Cuboid	18793	Bone (cortical)		1908	35.86
Cuneus	60164	Bone (cortical)		1908	114.79
Cystic duct[b]	1350		Bile	928	1.47
Deep fibular n.	951	Nerve		1075	1.02
Deltoid m.	228273	Muscle		1090	248.82
Dentate gyrus	721	Brain (gray matter)		1045	0.75
Descending colon	296281	Large intestine		1088	322.35
Diaphragm	228022	Diaphragm		1090	248.54
Digastric m.	7442	Muscle		1090	8.11
Distal phalanx (fifth)	348	Bone (cortical)		1908	0.66
Distal phalanx (fifth)	175	Bone (cortical)		1908	0.33
Distal phalanx (first)	2841	Bone (cortical)		1908	5.42
Distal phalanx (first)	155	Bone (cortical)		1908	0.30
Distal phalanx (fourth)	670	Bone (cortical)		1908	1.28
Distal phalanx (fourth)	524	Bone (cortical)		1908	1.00
Distal phalanx (second)	329	Bone (cortical)		1908	0.63
Distal phalanx (second)	1017	Bone (cortical)		1908	1.94
Distal phalanx (third)	1461	Bone (cortical)		1908	2.79
Distal phalanx (third)	333	Bone (cortical)		1908	0.64
Ear cartilage	3651	Cartilage		1100	4.02
Ear fat	16560	Fat		911	15.09
Ear skin	7285	Skin		1109	8.08
Epiglottis	777	Cartilage		1100	0.85
Esophagus[a]	27944	Esophagus	Muscle	1090	30.46
Extensor carpi radialis brevis m.	11621	Muscle		1090	12.67
Extensor carpi radialis longus m.	28681	Muscle		1090	31.26
Extensor carpi ulnaris m.	9698	Muscle		1090	10.57
Extensor digiti minimi m.	2427	Muscle		1090	2.65

Continued

Table 3. Continued

Structures	Number of voxel (A)	Structures of Virtual Population	[a]Substitution structures from Virtual Population	Density [kg/m^3] (B)	Weight (g) (A X B X 0.000001)
Extensor digitorum longus m.	28991	Muscle		1090	31.60
Extensor digitorum m.	21001	Muscle		1090	22.89
Extensor hallucis longus m.	5304	Muscle		1090	5.78
Extensor pollicis longus m.	5982	Muscle		1090	6.52
External acoustic meatus[b]	1163	Bone (cortical)		1908	2.22
External carotid a.	423	Blood		1050	0.44
External iliac a.	3203	Blood		1050	3.36
External jugular v.	3494	Blood		1050	3.67
External oblique abdominis m.	146052	Muscle		1090	159.20
Eye (choroid)	597	Blood		1050	0.63
Eye (cornea)	179	Eye (cornea)		1051	0.19
Eye (lens)	428	Eye (lens)		1076	0.46
Eye (retina)[b]	220	Nerve		1075	0.24
Eye (sclera)	567	Eye (sclera)		1032	0.59
Eye (vitreous humor)	12864	Eye (vitreous humor)		1005	12.93
Facial a.	565	Blood		1050	0.59
Fat	32369521	Fat		911	29488.63
Fat pad	884	Fat		911	0.81
Femoral n.	6498	Nerve		1075	6.99
Femur	846518	Bone (cortical)		1908	1615.16
Fibula	84632	Bone (cortical)		1908	161.48
Fibular collateral ligament	1070	Tendon/Ligament		1142	1.22
Fibularis brevis m.	77776	Muscle		1090	84.78
Fibularis longus m.	10045	Muscle		1090	10.95
Flexor carpi radialis m.	21378	Muscle		1090	23.30
Flexor carpi Ulnaris m.	22714	Muscle		1090	24.76
Flexor digiti minimi brevis m.	308	Muscle		1090	0.34
Flexor digitorum brevis m.	17047	Muscle		1090	18.58
Flexor digitorum longus m.	23022	Muscle		1090	25.09
Flexor digitorum profundus m.	11982	Muscle		1090	13.06
Flexor digitorum superficialis m.	11647	Muscle		1090	12.70

Continued

Table 3. Continued

Structures	Number of voxel (A)	Structures of Virtual Population	[a]Substitution structures from Virtual Population	Density [kg/m^3] (B)	Weight (g) (A X B X 0.000001)
Flexor hallucis longus m.	10034	Muscle		1090	10.94
Flexor pollicis brevis m.	554	Muscle		1090	0.60
Flexor pollicis longus m.	9378	Muscle		1090	10.22
Gall bladder	21013	Gallbladder		1071	22.50
Gastric a.	644	Blood		1050	0.68
Gastrocnemius m.	239943	Muscle		1090	261.54
Gastroduodenal a.	205	Blood		1050	0.22
Gastroepiploic a.	474	Blood		1050	0.50
Glenoid labrum	344	Tendon/Ligament		1142	0.39
Glossus m.	2891	Muscle		1090	3.15
Gluteus maximus m.	537591	Muscle		1090	585.97
Gluteus medius m.	341833	Muscle		1090	372.60
Gluteus minimus m.	118579	Muscle		1090	129.25
Gracilis m.	45521	Muscle		1090	49.62
Great cardiac v.	1212	Blood		1050	1.27
Hamate	3256	Bone (cortical)		1908	6.21
Heart	155112	Heart muscle		1081	167.68
Hepatic a.	399	Blood		1050	0.42
Hepatic v.	14576	Blood		1050	15.30
Hip bone	506619	Bone (cortical)		1908	966.63
Hippocampus[a]	2161	Hippocampus	Brain	1046	2.26
Humerus	218778	Bone (cortical)		1908	417.43
Hypophysis	726	Hypophysis		1053	0.76
Hypothalamus	665	Brain (gray matter)		1045	0.69
Iliacus m.	37747	Muscle		1090	41.14
Iliocostalis m.	160902	Muscle		1090	175.38
Iliopsoas m.	118963	Muscle		1090	129.67
Inferior alveolar a.	34	Blood		1050	0.04
Inferior frontal gyrus	36828	Brain (gray matter)		1045	38.49
Inferior lobar bronchus	21313	Bronchi		1102	23.49
Inferior mesenteric a.	349	Blood		1050	0.37

Continued

Table 3. Continued

Structures	Number of voxel (A)	Structures of Virtual Population	[a]Substitution structures from Virtual Population	Density [kg/m^3] (B)	Weight (g) (A X B X 0.000001)
Inferior oblique m.	460	Muscle		1090	0.50
Inferior obliquus capitis m.	11875	Muscle		1090	12.94
Inferior pulmonary v.	25872	Blood		1050	27.17
Inferior rectus m.	1000	Muscle		1090	1.09
Inferior temporal gyrus	9291	Brain (gray matter)		1045	9.71
Inferior vena cava	41794	Blood		1050	43.88
Infraorbital a.	62	Blood		1050	0.07
Infraspinatus m.	100805	Muscle		1090	109.88
Insula	13019	Brain (gray matter)		1045	13.60
Intercostal m.	91632	Muscle		1090	99.88
Intermediate cuneiform	6904	Bone (cortical)		1908	13.17
Internal carotid a.	2077	Blood		1050	2.18
Internal iliac a.	846	Blood		1050	0.89
Internal jugular v.	21555	Blood		1050	22.63
Internal oblique abdominis m.	82423	Muscle		1090	89.84
Interspinous ligament (L I–L II)	102	Tendon/Ligament		1142	0.12
Interspinous ligament (L II–L III)	205	Tendon/Ligament		1142	0.23
Interspinous ligament (L III–L IV)	117	Tendon/Ligament		1142	0.13
Interspinous ligament (L IV–L V)	60	Tendon/Ligament		1142	0.07
Interspinous ligament (L V–Sacrum)	40	Tendon/Ligament		1142	0.05
Intervertebral disc (Cii–iii)	924	Intervertebral disc		1100	1.02
Intervertebral disc (Ciii–iv)	1192	Intervertebral disc		1100	1.31
Intervertebral disc (Civ–v)	1171	Intervertebral disc		1100	1.29
Intervertebral disc (Cv–vi)	1245	Intervertebral disc		1100	1.37
Intervertebral disc (Cvi–vii)	1584	Intervertebral disc		1100	1.74
Intervertebral disc (Cvii–Ti)	1314	Intervertebral disc		1100	1.45
Intervertebral disc (Liii–Liv)	12417	Intervertebral disc		1100	13.66
Intervertebral disc (Lii–Liii)	9755	Intervertebral disc		1100	10.73
Intervertebral disc (Li–Lii)	6324	Intervertebral disc		1100	6.96
Intervertebral disc (Liv–Lv)	12849	Intervertebral disc		1100	14.13
Intervertebral disc (Lv–Sacrum)	9412	Intervertebral disc		1100	10.35

Continued

Table 3. Continued

Structures	Number of voxel (A)	Structures of Virtual Population	[a]Substitution structures from Virtual Population	Density [kg/m^3] (B)	Weight (g) (A X B X 0.000001)
Intervertebral disc (Ti–ii)	1220	Intervertebral disc		1100	1.34
Intervertebral disc (Tii–iii)	1348	Intervertebral disc		1100	1.48
Intervertebral disc (Tiii–iv)	1456	Intervertebral disc		1100	1.60
Intervertebral disc (Tiv–v)	1424	Intervertebral disc		1100	1.57
Intervertebral disc (Tv–vi)	1725	Intervertebral disc		1100	1.90
Intervertebral disc (Tvi–vii)	1929	Intervertebral disc		1100	2.12
Intervertebral disc (Tvii–viii)	2018	Intervertebral disc		1100	2.22
Intervertebral disc (Tviii–ix)	2068	Intervertebral disc		1100	2.27
Intervertebral disc (Tix–x)	2625	Intervertebral disc		1100	2.89
Intervertebral disc (Tx–Txi)	2769	Intervertebral disc		1100	3.05
Intervertebral disc (Txi–Txii)	3715	Intervertebral disc		1100	4.09
Intervertebral disc (Txii–Li)	5408	Intervertebral disc		1100	5.95
Kidney	270722	Kidney		1066	288.59
Lat cuneiform	8350	Bone (cortical)		1908	15.93
Lateral cricoarytenoid m.	152	Muscle		1090	0.17
Lateral mandibular incisor tooth	581	Tooth		2180	1.27
Lateral maxillary incisor tooth	504	Tooth		2180	1.10
Lateral meniscus	1939	Meniscus		1100	2.13
Lateral occipital gyrus	4401	Brain (gray matter)		1045	4.60
Lateral occipitotemporal gyrus	10257	Brain (gray matter)		1045	10.72
Lateral orbital gyrus	7788	Brain (gray matter)		1045	8.14
Lateral pterygoid m.	10026	Muscle		1090	10.93
Lateral rectus m.	1277	Muscle		1090	1.39
Latissimus dorsi m.	218394	Muscle		1090	238.05
Left atrium	20052	Heart lumen		1050	21.05
Left coronary a.	562	Blood		1050	0.59
Left ventricle	90170	Heart lumen		1050	94.68
Levator palpebrae superioris m.	924	Muscle		1090	1.01
Levator scapulae m.	33975	Muscle		1090	37.03
Ligamentum flavum (L I–L II)	1025	Tendon/Ligament		1142	1.17
Ligamentum flavum (L II–L III)	1762	Tendon/Ligament		1142	2.01

Continued

Table 3. Continued

Structures	Number of voxel (A)	Structures of Virtual Population	[a]Substitution structures from Virtual Population	Density [kg/m^3] (B)	Weight (g) (A X B X 0.000001)
Ligamentum flavum (L III–L IV)	1901	Tendon/Ligament		1142	2.17
Ligamentum flavum (L IV–L V)	1834	Tendon/Ligament		1142	2.09
Ligamentum flavum (L V–Sacrum)	1898	Tendon/Ligament		1142	2.17
Lingual a.	257	Blood		1050	0.27
Lingual gyrus	3468	Brain (gray matter)		1045	3.62
Liver	869590	Liver		1079	938.29
Longissimus m.	179298	Muscle		1090	195.43
Longus capitis m.	9903	Muscle		1090	10.79
Lumbar vetebra (fifth)	40395	Bone (cortical)		1908	77.07
Lumbar vetebra (fourth)	38547	Bone (cortical)		1908	73.55
Lumbar vetebrae (first)	29404	Bone (cortical)		1908	56.10
Lumbar vetebrae (second)	33096	Bone (cortical)		1908	63.15
Lumbar vetebrae (third)	39001	Bone (cortical)		1908	74.41
Lunate	2897	Bone (cortical)		1908	5.53
Lung	1352390	Lung		394	532.84
Main bronchus	7437	Bronchi		1102	8.20
Mandible	50404	Mandible		1908	96.17
Mandibular canine tooth	919	Tooth		2180	2.00
Mandibular premolar tooth (first)	803	Tooth		2180	1.75
Mandibular premolar tooth (second)	621	Tooth		2180	1.35
Manubrium	15754	Bone (cortical)		1908	30.06
Masseter m.	25610	Muscle		1090	27.91
Maxillary a.	269	Blood		1050	0.28
Maxillary canine tooth	923	Tooth		2180	2.01
Maxillary premolar tooth (first)	905	Tooth		2180	1.97
Maxillary premolar tooth (first)	1794	Tooth		2180	3.91
Maxillary premolar tooth (second)	852	Tooth		2180	1.86
Maxillary premolar tooth (second)	2783	Tooth		2180	6.07
Med cuneiform	15818	Bone (cortical)		1908	30.18
Medial frontal gyrus	28105	Brain (gray matter)		1045	29.37
Medial mandibular incisor tooth	413	Tooth		2180	0.90

Continued

Table 3. Continued

Structures	Number of voxel (A)	Structures of Virtual Population	[a]Substitution structures from Virtual Population	Density [kg/m^3] (B)	Weight (g) (A X B X 0.000001)
Medial maxillary incisor tooth	667	Tooth		2180	1.45
Medial meniscus	1807	Meniscus		1100	1.99
Medial occipital gyrus	4776	Brain (gray matter)		1045	4.99
Medial occipitotemporal gyrus	2325	Brain (gray matter)		1045	2.43
Medial orbital gyrus	5784	Brain (gray matter)		1045	6.04
Medial pterygoid m.	8982	Muscle		1090	9.79
Medial rectus m.	1284	Muscle		1090	1.40
Median n.	3459	Nerve		1075	3.72
Medulla oblongata	3131	Medulla oblongata		1046	3.28
Metacarpal bone (fifth)	5179	Bone (cortical)		1908	9.88
Metacarpal bone (first)	7079	Bone (cortical)		1908	13.51
Metacarpal bone (fourth)	6089	Bone (cortical)		1908	11.62
Metacarpal bone (second)	9796	Bone (cortical)		1908	18.69
Metacarpal bone (third)	8595	Bone (cortical)		1908	16.40
Metatarsal bone (fifth)	13131	Bone (cortical)		1908	25.05
Metatarsal bone (first)	26614	Bone (cortical)		1908	50.78
Metatarsal bone (fourth)	11311	Bone (cortical)		1908	21.58
Metatarsal bone (second)	12346	Bone (cortical)		1908	23.56
Metatarsal bone (third)	11393	Bone (cortical)		1908	21.74
Midbrain	1993	Midbrain		1046	2.08
Middle cardiac v.	175	Blood		1050	0.18
Middle frontal gyrus	57506	Brain (gray matter)		1045	60.09
Middle lobar bronchus	2756	Cartilage		1100	3.03
Middle meningeal a.	524	Blood		1050	0.55
Middle phalanx (fifth)	745	Bone (cortical)		1908	1.42
Middle phalanx (fifth)	562	Bone (cortical)		1908	1.07
Middle phalanx (fourth)	1728	Bone (cortical)		1908	3.30
Middle phalanx (fourth)	474	Bone (cortical)		1908	0.90
Middle phalanx (second)	1127	Bone (cortical)		1908	2.15
Middle phalanx (second)	852	Bone (cortical)		1908	1.63
Middle phalanx (third)	1194	Bone (cortical)		1908	2.28

Continued

Table 3. Continued

Structures	Number of voxel (A)	Structures of Virtual Population	[a]Substitution structures from Virtual Population	Density [kg/m^3] (B)	Weight (g) (A X B X 0.000001)
Middle phalanx (third)	701	Bone (cortical)		1908	1.34
Middle scalenus m.	4780	Muscle		1090	5.21
Middle temporal gyrus	27251	Brain (gray matter)		1045	28.48
Multifidus m.	175737	Muscle		1090	191.55
Mylohyoid m.	3489	Muscle		1090	3.80
Nasal cavity	19899	Mucous membrane		1102	21.93
Navicular	14988	Bone (cortical)		1908	28.60
Oblique arytenoid m.	124	Muscle		1090	0.14
Obturator n.	2780	Nerve		1075	2.99
Occipital a.	183	Blood		1050	0.19
Opponens digiti minimi m.	1659	Muscle		1090	1.81
Opponens pollicis m.	12707	Muscle		1090	13.85
Optic nerve	1559	Nerve		1075	1.68
Oral cavity	8662	Air		1	0.01
Oral mucosa	8078	Mucous membrane		1102	8.90
Ovary	15354	Ovary		1048	16.09
Palmaris longus m.	36394	Muscle		1090	39.67
Pancreas	45999	Pancreas		1087	50.00
Paracentral lobule	5827	Brain (gray matter)		1045	6.09
Parahippocampal gyrus	16530	Brain (gray matter)		1045	17.27
Parotid gland	32171	Salivary gland		1048	33.72
Patella	30913	Bone (cortical)		1908	58.98
Pectoralis major m.	178577	Muscle		1090	194.65
Pectoralis minor m.	31075	Muscle		1090	33.87
Pharynx	6292	Pharynx		1	0.01
Pineal body	51	Pineal body		1053	0.05
Pisiform	823	Bone (cortical)		1908	1.57
Pons	8168	Pons		1046	8.54
Popliteus m.	14288	Muscle		1090	15.57
Portal v.	7031	Blood		1050	7.38
Postcentral gyrus	46473	Brain (gray matter)		1045	48.56

Continued

Table 3. Continued

Structures	Number of voxel (A)	Structures of Virtual Population	[a]Substitution structures from Virtual Population	Density [kg/m^3] (B)	Weight (g) (A X B X 0.000001)
Posterior auricular a.	75	Blood		1050	0.08
Posterior commissure	5	Commissura posterior		1041	0.01
Posterior cricoarytenoid m.	596	Muscle		1090	0.65
Posterior cruciate ligament	2922	Tendon/Ligament		1142	3.34
Posterior rectus capitis major m.	7040	Muscle		1090	7.67
Posterior rectus capitis minor m.	2689	Muscle		1090	2.93
Posterior scalenus m.	9098	Muscle		1090	9.92
Precentral gyrus	50331	Brain (gray matter)		1045	52.60
Precuneus	20237	Brain (gray matter)		1045	21.15
Pronator quadratus m.	4578	Muscle		1090	4.99
Pronator teres m.	15996	Muscle		1090	17.44
Proper hepatic a.	74	Blood		1050	0.08
Proximal phalanx (fifth)	2376	Bone (cortical)		1908	4.53
Proximal phalanx (fifth)	2043	Bone (cortical)		1908	3.90
Proximal phalanx (first)	4805	Bone (cortical)		1908	9.17
Proximal phalanx (first)	9465	Bone (cortical)		1908	18.06
Proximal phalanx (fourth)	3799	Bone (cortical)		1908	7.25
Proximal phalanx (fourth)	1917	Bone (cortical)		1908	3.66
Proximal phalanx (second)	4338	Bone (cortical)		1908	8.28
Proximal phalanx (second)	2705	Bone (cortical)		1908	5.16
Proximal phalanx (third)	4932	Bone (cortical)		1908	9.41
Proximal phalanx (third)	2346	Bone (cortical)		1908	4.48
Psoas major m.	91118	Muscle		1090	99.32
Pulmonary a.	38726	Blood		1050	40.66
Pulmonary trunk	17110	Blood		1050	17.97
Quadratus lumborum m.	30803	Muscle		1090	33.58
Radial n.	2672	Nerve		1075	2.87
Radius	61730	Bone (cortical)		1908	117.78
Rectum	54295	Large intestine		1088	59.07
Rectus abdominis m.	110433	Muscle		1090	120.37
Rectus capitis lateralis m.	1098	Muscle		1090	1.20

Continued

Table 3. Continued

Structures	Number of voxel (A)	Structures of Virtual Population	[a]Substitution structures from Virtual Population	Density [kg/m^3] (B)	Weight (g) (A X B X 0.000001)
Rectus femoris m.	148671	Muscle		1090	162.05
Rhomboid major m.	47283	Muscle		1090	51.54
Rhomboid minor m.	5297	Muscle		1090	5.77
Rib (first)	10350	Bone (cortical)		1908	19.75
Rib (second)	18344	Bone (cortical)		1908	35.00
Rib (third)	20509	Bone (cortical)		1908	39.13
Rib (fourth)	24891	Bone (cortical)		1908	47.49
Rib (fifth)	27383	Bone (cortical)		1908	52.25
Rib (sixth)	29431	Bone (cortical)		1908	56.15
Rib (seventh)	24913	Bone (cortical)		1908	47.53
Rib (eighth)	22004	Bone (cortical)		1908	41.98
Rib (ninth)	17114	Bone (cortical)		1908	32.65
Rib (tenth)	8424	Bone (cortical)		1908	16.07
Ribs	50154	Bone (cortical)		1908	95.69
Right atrium	112214	Heart lumen		1050	117.82
Right coronary a.	415	Blood		1050	0.44
Right ventricle	165864	Heart lumen		1050	174.16
Sacrum	148765	Bone (cortical)		1908	283.84
Sartorius m.	83377	Muscle		1090	90.88
Scaphoid	3736	Bone (cortical)		1908	7.13
Scapula	85330	Bone (cortical)		1908	162.81
Sciatic n.	10298	Nerve		1075	11.07
Semimembranosus m.	168651	Muscle		1090	183.83
Semitendinosus m.	106725	Muscle		1090	116.33
Sigmoid colon	101543	Large intestine		1088	110.48
Skin	1558967	Skin		1109	1728.89
Small intestine[a]	694251	Small intestine	Urinary bladder wall	1086	753.96
Soleus m.	348105	Muscle		1090	379.43
Spinal cord	22742	Spinal cord		1075	24.45
Spinalis m.	10899	Muscle		1090	11.88
Spleen	121485	Spleen		1089	132.30

Continued

Table 3. Continued

Structures	Number of voxel (A)	Structures of Virtual Population	[a]Substitution structures from Virtual Population	Density [kg/m^3] (B)	Weight (g) (A X B X 0.000001)
Splenic a.	1884	Blood		1050	1.98
Sternocleidomastoid m.	53011	Muscle		1090	57.78
Sternohyoid m.	9184	Muscle		1090	10.01
Sternothyroid m.	5140	Muscle		1090	5.60
Sternum	18055	Bone (cortical)		1908	34.45
Stomach[a]	499500	Stomach	Urinary bladder wall	1086	542.46
Straight gyrus	14223	Brain (gray matter)		1045	14.86
Subclavian a.	2381	Blood		1050	2.50
Subclavian v.	3638	Blood		1050	3.82
Subclavius m.	5075	Muscle		1090	5.53
Sublingual gland	4933	Salivary gland		1048	5.17
Submandibular gland	11051	Salivary gland		1048	11.58
Subscapularis m.	130233	Muscle		1090	141.95
Superficial fibular n.	188	Nerve		1075	0.20
Superficial temporal a.	195	Blood		1050	0.20
Superior alveolar a.	80	Blood		1050	0.08
Superior frontal gyrus	85647	Brain (gray matter)		1045	89.50
Superior laryngeal a.	33	Blood		1050	0.03
Superior lobar bronchus	10635	Bronchi		1102	11.72
Superior mesenteric a.	617	Blood		1050	0.65
Superior oblique m.	388	Muscle		1090	0.42
Superior obliquus capitis m.	2895	Muscle		1090	3.16
Superior parietal lobule	34949	Brain (gray matter)		1045	36.52
Superior pulmonary v.	14837	Blood		1050	15.58
Superior rectus m.	842	Muscle		1090	0.92
Superior temporal gyrus	45679	Brain (gray matter)		1045	47.73
Superior thyroid a.	122	Blood		1050	0.13
Superior vena cava	12572	Blood		1050	13.20
Supinator m.	18636	Muscle		1090	20.31
Supramarginal gyrus	44823	Brain (gray matter)		1045	46.84
Supraspinatus m.	51211	Muscle		1090	55.82

Continued

Table 3. Continued

Structures	Number of voxel (A)	Structures of Virtual Population	[a]Substitution structures from Virtual Population	Density [kg/m^3] (B)	Weight (g) (A X B X 0.000001)
Talus	52202	Bone (cortical)		1908	99.60
Temporal m.	27919	Muscle		1090	30.43
Teres major	54497	Muscle		1090	59.40
Teres minor	26438	Muscle		1090	28.82
Thalamus[a]	7953	Thalamus	Brain	1046	8.32
Thoracic aorta	25576	Blood		1050	26.85
Thoracic vertebra (eighth)	17340	Bone (cortical)		1908	33.08
Thoracic vertebra (eleventh)	23400	Bone (cortical)		1908	44.65
Thoracic vertebra (fifth)	13372	Bone (cortical)		1908	25.51
Thoracic vertebra (first)	5411	Bone (cortical)		1908	10.32
Thoracic vertebra (fourth)	12310	Bone (cortical)		1908	23.49
Thoracic vertebra (ninth)	18996	Bone (cortical)		1908	36.24
Thoracic vertebra (second)	13616	Bone (cortical)		1908	25.98
Thoracic vertebra (seventh)	15454	Bone (cortical)		1908	29.49
Thoracic vertebra (sixth)	13679	Bone (cortical)		1908	26.10
Thoracic vertebra (tenth)	20711	Bone (cortical)		1908	39.52
Thoracic vertebra (third)	11471	Bone (cortical)		1908	21.89
Thoracic vertebra (Twelfth)	26518	Bone (cortical)		1908	50.60
Thyroarytenoid m.	182	Muscle		1090	0.20
Thyroepiglottic ligament	351	Tendon/Ligament		1142	0.40
Thyrohyoid membrane[b]	616		Tendon/Ligament	1142	0.68
Thyroid cartilage	2673	Cartilage		1100	2.94
Thyroid gland[a]	13668	Thyroid gland	Salivary gland	1048	14.32
Tibia	521767	Bone (cortical)		1908	995.53
Tibial collateral ligament	3055	Tendon/Ligament		1142	3.49
Tibial n.	21192	Nerve		1075	22.78
Tibialis ant m.	119642	Muscle		1090	130.41
Tibialis post m.	92482	Muscle		1090	100.81
Tongue	42563	Tongue		1090	46.39
Trachea[a]	17447	Trachea	Bronchi	1102	19.23
Transverse arytenoid m.	293	Muscle		1090	0.32

Continued

Table 3. Continued

Structures	Number of voxel (A)	Structures of Virtual Population	[a]Substitution structures from Virtual Population	Density [kg/m^3] (B)	Weight (g) (A X B X 0.000001)
Transverse colon	234107	Large intestine		1088	254.71
Transverse temporal gyrus	3259	Brain (gray matter)		1045	3.41
Transversospinales m.	43523	Muscle		1090	47.44
Transversus abdominis m.	66948	Muscle		1090	72.97
Trapezium	2271	Bone (cortical)		1908	4.33
Trapezius m.	160098	Muscle		1090	174.51
Trapezoid	1951	Bone (cortical)		1908	3.72
Triceps brachii m.	195011	Muscle		1090	212.56
Tricuspid valve	89		Cartilage	1100	0.10
Triquetrum	1575	Bone (cortical)		1908	3.01
Ulna	62956	Bone (cortical)		1908	120.12
Ulnar n.	2854	Nerve		1075	3.07
Uncus	4229	Brain (gray matter)		1045	4.42
Ureter[a]	5487	Ureter/Urethra	Urinary bladder wall	1086	5.96
Urethra[a]	83	Ureter/Urethra	Urinary bladder wall	1086	0.09
Urinary bladder	76323	Urinary bladder wall		1086	82.89
Uterine tube[b]	8885		Urinary bladder wall	1086	9.65
Uterus[a]	55035	Uterus	Urinary bladder wall	1086	59.77
Vagina	5396	Vagina		1088	5.87
Vastus intermedius m.	483776	Muscle		1090	527.32
Vastus lateralis m.	417476	Muscle		1090	455.05
Vastus medialis m.	193694	Muscle		1090	211.13
Vestibular fold[b]	289		Tendon/Ligament	1142	0.33
Vocal fold[b]	139		Tendon/Ligament	1142	0.16
Vocal ligament	75		Tendon/Ligament	1142	0.09
		Total number		459	
		Total weight		56 kg	

a. = artery, m. = muscle; n. = nerve, v. = vein.
[a]Change in the structure of the optimal density from the list of Virtual Population (2017) because the density of structures in Virtual Population was incorrect.
[b]Assigned to the most similar structure(s) in Virtual Population (2017) because there was no such structure on that list.

DISCUSSION

Of all the source materials available for designing a phantom for virtually testing electromagnetic dosimetry, segmented images based on the sectioned images from the Visible Human Project (VHP) [21], VK [15, 16, 22], and Visible Chinese Human (VCH) [23] are most appropriate because detailed structures of the human body can be distinguished in real color (>24 bits color) and high resolution (< 0.2-mm^3 voxels), compared with CT and MRI [3–6]. However, other

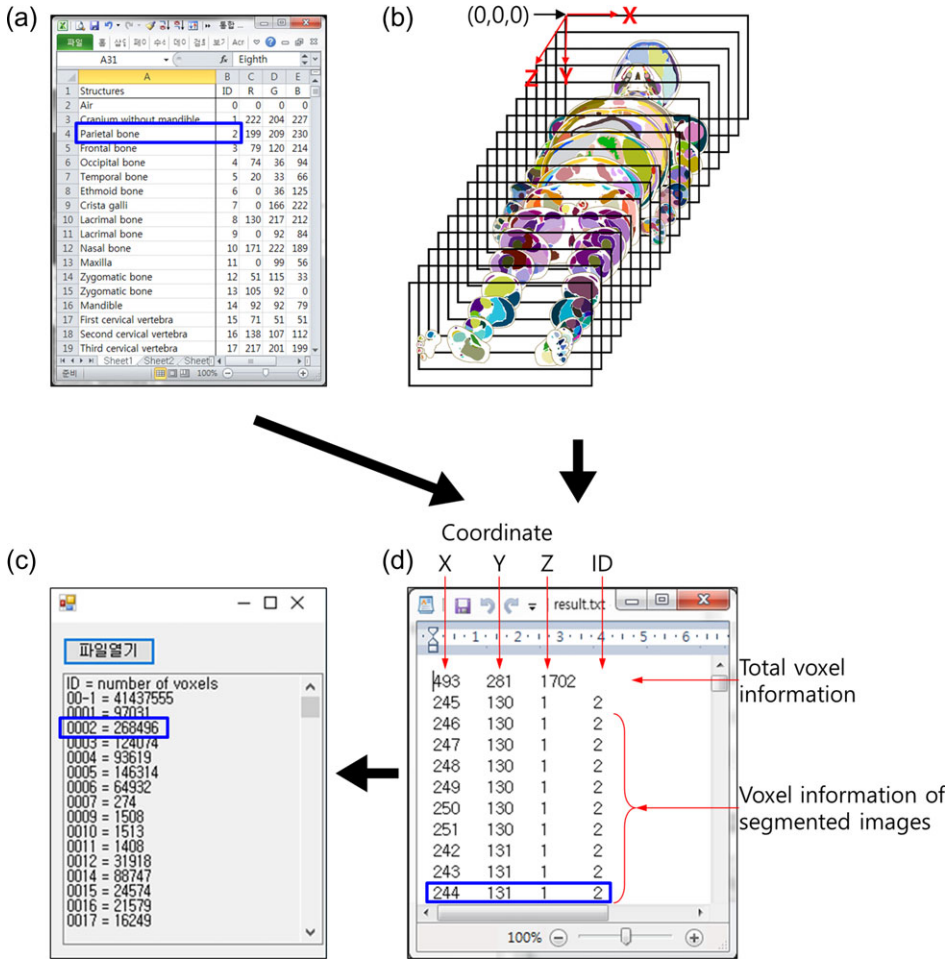

Fig. 2. Process of acquiring voxel information from segmented images. (a) ID numbers were assigned serially to all segmented structures. (b) After segmented images were stacked in the computer memory, (c) voxel information (*x*, *y* and *z* coordinates and the ID number of each segmented structure) for a phantom was produced and saved in TXT format using VK-phantom.jar software. (d) The voxel number in the phantom was counted according to ID numbers using String_analysis.exe. For example, for the Blue box in (a), (c), and (d)), the voxel number of ID 2 (parietal bone) was 268,496.

researchers have not been able to produce phantoms based on the original properties of the source materials, even when high-resolution sectioned images were used [3–6, 8, 24, 25]. In this study, we aimed to produce a VK-phantom male and female with properties closely resembling the original properties of the source materials (Table 1).

Tissues with different features should be distinguishable in detail in a phantom. In a phantom study, classification by tissue features rather than detailed structures is important. However, if a phantom does not have detailed structure, the phantom is unreliable because different tissues can be regarded as the same. In other phantom studies, including Virtual Family and ICRP publications, the muscles and their surrounding structures in the upper and lower limbs were not differentiated, although they are different tissues. In the orbit, the small vessels are not distinguished, although radiation can have differentially damaging effects on the various small vessels. In addition, many structures were not differentiated in other studies [1, 4, 5, 7, 14]. Therefore, in this study, a VK-phantom male with 583 structures and a VK-phantom female with 459 structures were constructed, and both were determined to be reliable in terms of their detailed structures (Tables 1–3).

Even tissues with identical features should be differentiated in a phantom, as well as tissues with different features. In dosimetry study on the possible effects of radiofrequency fields, particularly given the popularity of mobile phone use, the cerebrum is considered a very important organ in terms of identifying any possible associations between radiofrequency electromagnetic fields, including those from mobile phones, and brain tumors [26, 27]. To investigate such possible associations, the area exposed to these fields must be precisely determined, and a exact structure name area must be noted. In earlier studies, the cerebrum was regarded as comprising only two tissues: gray and white matter [1, 3–5, 20]. Therefore, we used VK-phantoms in which the cerebrum was divided along each gyrus (Tables 2, 3) [18, 22], and the absorption of each area was described and measured quantitatively.

Table 4. Comparison of VK phantom male, HDRK-man, ICRP male and Virtual Family after each structure has been rearranged according to the list of structures in Virtual Population (2017)

VK-phantom			HDRK-man (Kim *et al.* [5])		ICRP male phantom (Christ *et al.* [1])		Virtual Family (Duke) (Christ *et al.* [1])	
Structures	Weight (g)	Number	Structures	Weight (g)	Structures	Weight (g)	Structures	Weight (g)
Adrenal gland	0	0	Adrenal	14	Adrenal gland	14	Adrenal glands	11
Bile	1	1			Gall bladder contents	54.1		
Blood	531	91	Blood	254	Blood	371.5		
Blood vessel wall	6	9						
Bone (cortical)	10 091	90	Bone (cortical)	9607	Skeleton	10450	Skeleton	7900
Bone marrow (red)	0	0	Bone (marrow_infiltrated)	1068			Red bone marrow	960
Brain	1635	5	Brain	1620	Brain	1450	Brain	1370
Brain (gray matter)	43	5						
Brain (white matter)	1	1					Esophagus (wall)	56
Breast gland	0	0			Breast, glandular tissue	10		
Bronchi	36	18						
Bronchial lumen	0	0			Breast, adipose tissue	15		
Cartilage	8	6						
Cerebellum	175	1						
Cerebrospinal fluid	241	2						
Diaphragm	333	1						
Ductus deferens	3	1						
Epididymis	11	1						
Esophagus			Esophagus	40	Esophagus	40		
Eye (cornea)	0.02	1			Prostate	17		
Eye (lens)	1	1	Eye (lens)	0.51	Lens	0.4	Lens	0.3
Eye (sclera)	1	1						
Eye (vitreous humor)	15	1	Eye	21	Eyes	15		
Fat	8187	1	Fat	23 400.2			Adipose tissue	11 800
Gallbladder	129	1	Gall bladder, Bile	13	Gall bladder wall	13.9	Gall bladder (wall + contents)	19

Continued

Table 4. Continued

VK-phantom			HDRK-man (Kim *et al.* [5])		ICRP male phantom (Christ *et al.* [1])		Virtual Family (Duke) (Christ *et al.* [1])	
Structures	Weight (g)	Number	Structures	Weight (g)	Structures	Weight (g)	Structures	Weight (g)
Heart lumen	207	2			Heart contents (blood)	510		
Heart muscle	606	3	Heart wall	391	Heart wall	330	Heart	750
Hypophysis	1	2			Pituitary gland	0.6		
Intervertebral Disc	174	23						
Kidney	433	1	Kidney	359	Kidneys	310	Kidney	360
Kidney (cortex)	0	0						
Kidney (medulla)	0	0						
Large intestine	748	8	Large intestine	343	Large intestinal wall	370	Colon wall	530
Large intestinal lumen					Large intestinal contents	300		
Larynx	0	0						
Liver	2186	1	Liver	1417	Liver	1800	Liver	1240
Lung	2190	1			Lungs	1200	Lung	3800
Lung (deflated)	0	0	Lung (deflated/inflated)	1156				
Mandible	169	1	Breast	23.3				
Meniscus	1	2						
Mucous membrane	0	0	Oral mucosa	21	Oral mucosa	35.8		
Muscle	22 955	170	Muscle	23 300	Muscle	29 000	Muscle	34 100
Nerve	81	37	Nerve					
Pancreas	124	1	Pancreas	126	Pancreas	140	Pancreas	70
Pharynx	0	1						
Prostate	12	1	Prostate	12				
Salivary gland	78	3	Salivary gland	87	Salivary glands	85		
Seminal vesicle	4	1						
Skin	1786	1	Skin	4260	Skin	3728	Skin	5500
Skull cancellous	0	0						
Skull cortical	1519	8						

Continued

Table 4. Continued

VK-phantom			HDRK-man (Kim *et al.* [5])		ICRP male phantom (Christ *et al.* [1])		Virtual Family (Duke) (Christ *et al.* [1])	
Structures	Weight (g)	Number	Structures	Weight (g)	Structures	Weight (g)	Structures	Weight (g)
Small intestine	703	2	Small intestine	602	Small intestinal wall	650	Small intestinal wall	630
Small intestinal lumen					Small Intestine contents	350		
Spinal cord	43	1	Spinal cord					
Spleen	1111	1	Spleen	177	Spleen	150	Spleen	150
Stomach		1	Stomach	141	Stomach wall	150		
Stomach lumen	207	1			Stomach contents	250		
Tendon/Ligament	49	22						
Testis	25	1	Testis		Testis	35	Testis	18
Thalamus	24	1						
Thymus	0	0	Thymus	39	Thymus	25	Thymus	4
Thyroid gland	18	1	Thyroid	15	Thyroid	20	Thyroid	9
Tongue	50	1	Tongue		Tongue	73		
Tooth	39	14	Tooth		Tooth	50	Tooth	31
Trachea	28	1			Trachea	10		
Ureter/Urethra	3	3			Ureters	16		
Urinary bladder wall	45	1	Urinary bladder	42	Urinary bladder wall	50		
Urine	4	1			Urinary bladder contents	200		
Vertebrae	1022	19						
					Tonsils	3		
					Extrathoracic region	39.4		
			Gonad	28	Lymphatic nodes	138		
			Extrathoracic region	73	Residual tissue	20 458.4		
Total weight	58 kg			68 kg		72 kg		69 kg

Furthermore, in most phantoms, accurate anatomical terms have not been used, even though this can result in incorrect descriptions of tissue features in the phantom, rendering the phantoms unreliable. For example, in some studies, the authors have referred to the thyroid, but it is unclear whether the tissue being referred to is the thyroid gland or the thyroid cartilage (Table 4) [1, 4–6]. Official terminology from *Terminologia Anatomica* should be used [28], as in this study (Tables 2, 3).

The tissue density of Virtual Population [11] is the most reliable of all the phantom studies. Nevertheless, some of the Virtual Population densities are unreliable. The density of the small intestine (1030 kg/m^3) is between that of the bone marrow (red) (1029 kg/m^3) and eye (sclera) (1032 kg/m^3), although they are very different tissues; the small intestine consists of a mucous membrane, smooth muscle, vessels, and connective tissue, whereas the bone marrow (red) and eye (sclera) have densities similar to the blood and mucous membrane, respectively. The densities of the brain (gray matter), prostate, and seminal vesicles were identical (1045 kg/m^3), even though the tissue features of the structures are not identical. The density of the blood vessel wall, bronchi, and penis were identical (1102 kg/m^3), although the blood vessel wall, bronchi, and penis consist of smooth muscles with various connective tissues, cartilage with some smooth muscle, and blood in various connective tissues, respectively. In addition, in ICRP and HDRK [1, 4, 5], the density of each structure was not normal. Therefore, the densities of some structures were rearranged based on Virtual Population (marked with a superscript 'a' on Tables 2, 3).

Although the densities of the structures were rearranged or newly assigned, they were not accurate, because 104 tissue densities noted in Virtual Population could not be assigned to the 583 structures of the VK-phantom male and the 459 structures of the VK-phantom female. Therefore, in the near future, the densities of all detailed structures will need to be measured.

The voxel size of a phantom with detailed structures should definitely be small enough to accurately measure the effects of electromagnetic radiation. In the case of the VHP female phantom (voxel size, 6 × 6 × 6 mm^3) [3] and the VCH female phantom (voxel size, 2 × 2 × 4 mm^3) [6], the voxel size of the source images could not be used (VHP female, 0.33 mm^3 ; VCH female, 0.2 mm^3). In the case of the HDRK man [5] and the HDRK woman [4], phantoms of 2-mm^3-sized voxels were made, even though the source images had 0.2-mm^3-sized voxels [15–17]. In our preliminary test, we generated a phantom of the whole body (file size, 500 GB) from images of the original voxel size (0.2 mm^3); consequently, the phantom could never be analyzed on a personal computer. Therefore, we constructed phantoms with 1-mm^3-sized voxels, which is notably smaller than the voxel size of the phantoms described previously. As a result, very small structures could be observed in the VK-phantoms (e.g. sinu-atrial nodal branch, six voxels and 0.006 g; Table 1).

In the most recent studies, voxel phantoms are made of polygonal surface models based on MRI, CT, or sectioned images because polygonal surface models have several merits [1, 3–5, 20]. However, a VK-phantom male could never be made using polygonal surface modeling for the following reasons. First, a phantom with 583 structures comprises many polygons, even if it is based on low-resolution images (voxel size, >1-mm^3); consequently, the phantom could not be handled on a personal computer, even if the newest hardware and software were used. Second, polygonal surface models are deficient in that all of the information from the source images is not incorporated. When pixels of segmented images are reconstructed into polygonal surface models, the outer shapes of the models are smoothed. When polygonal surface models are converted into voxel models, the outer edges of the models are angulated. Because of the smoothing and angulating procedures, voxel information from the source images is lost [20]. Therefore, in this study, segmented images (1-mm^3-sized voxels) were converted directly into voxel models (VK-phantoms) in TXT format using house-developed software (VK-phantom.jar), without polygonal surface models.

Please note, voxel information in the VK-phantoms cannot be analyzed using commercial software for a virtual radiation test, because the dataset for a VK-phantom with a 1-mm^3-sized voxel is ~1 GB or more in size. Consequently, house-developed software (String_analysis.exe) was designed to analyze voxel information in the phantom.

In this study, a 583-structure VK-phantom male and a 459-structure VK-phantom female were constructed. In the VK-phantoms, voxel information of the whole body could be analyzed in detail (Tables 2, 3) by virtue of accurate segmentation, detailed structures, and small voxel size [15–18]. We continue to make new segmented images with new structures from the high-resolution sectioned images of VK. However, the new segmented images cannot be reconstructed into voxel models via polygonal surface modeling on even the newest personal computer. Therefore, future work will focus on converting convenient polygonal surface models into voxel models. For this work, improved surface modeling methods based on the segmented images [29] will be developed. Furthermore, the size of each structure in the VK-phantoms should be standardized. If the VK-phantoms are standardized and the mass density of each structure is precise, researchers will be able to measure the exact absorption in specific organs and tissues in the whole body. The segmented images and the house-developed software described in this study are distributed free of charge at neuroanatomy.kr even though most phantoms, including Virtual Population, are not free.

ACKNOWLEDGEMENTS

We thank the Korea Institute of Science and Technology Information of Republic of Korea for allowing the use of the sectioned images of Visible Korean (http://vkh3.kisti.re.kr).

CONFLICT OF INTEREST

The authors state that there is no conflict of interest.

FUNDING

This work was supported by the IT R&D program of MSIP/IITP [B0138-16-1002, Study on the EMF exposure control in smart society].

REFERENCES

1. Christ A, Kainz W, Hahn EG et al. The Virtual Family—development of surface-based anatomical models of two adults and two children for dosimetric simulations. *Phys Med Biol* 2010;55: N23–38.

2. Lee A-K, Byun J-K, Park JS et al. Development of 7-year-old Korean child model for computational dosimetry. *ETRI J* 2009; 31:237–9.
3. Yanamadala J, Noetscher GM, Rathi VK et al. New VHP-Female v. 2.0 full-body computational phantom and its performance metrics using FEM simulator ANSYS HFSS. *Conf Proc IEEE Eng Med Biol Soc* 2015;2015:3237–41.
4. Yeom YS, Jeong JH, Kim CH et al. HDRK-Woman: whole-body voxel model based on high-resolution color slice images of Korean adult female cadaver. *Phys Med Biol* 2014;59:3969–84.
5. Kim CH, Choi SH, Jeong JH et al. HDRK-Man: a whole-body voxel model based on high-resolution color slice images of a Korean adult male cadaver. *Phys Med Biol* 2008;53:4093–106.
6. Sun W, Jia X, Xie T et al. Construction of boundary-surface-based Chinese female astronaut computational phantom and proton dose estimation. *J Radiat Res* 2013;54:383–97.
7. Xu XG. An exponential growth of computational phantom research in radiation protection, imaging, and radiotherapy: a review of the fifty-year history. *Phys Med Biol* 2014;59:R233–302.
8. Segars WP, Sturgeon G, Mendonca S et al. 4D XCAT phantom for multimodality imaging research. *Med Phys* 2010;37:4902–15.
9. Menzel HG, Clement C, DeLuca P. Realistic reference phantoms: an ICRP/ICRU joint effort. A report of adult reference computational phantoms. ICRP Publication 110. *Ann ICRP* 2009;39:1–164.
10. Schlattl H, Zankl M, Petoussi-Henss N. Organ dose conversion coefficients for voxel models of the reference male and female from idealized photon exposures. *Phys Med Biol* 2007;52:2123–45.
11. IT'IS. *Virtual Population*. https://www.itis.ethz.ch/virtual-population/tissue-properties/database/density/ (1 March 2018, date last accessed)
12. Gabriel C, Gabriel S, Corthout E. The dielectric properties of biological tissues: I. Literature survey. *Phys Med Biol* 1996;41: 2231–49.
13. The 2007 Recommendations of the International Commission on Radiological Protection. ICRP Publication 103. *Ann ICRP* 2007;37:1–332.
14. Basic anatomical and physiological data for use in radiological protection: reference values. A report of age- and gender-related differences in the anatomical and physiological characteristics of reference individuals. ICRP Publication 89. *Ann ICRP* 2002;32: 5–265.
15. Park JS, Chung MS, Hwang SB et al. Visible Korean human: improved serially sectioned images of the entire body. *IEEE Trans Med Imaging* 2005;24:352–60.
16. Park HS, Choi DH, Park JS. Improved sectioned images and surface models of the whole female body. *Int J Morphol* 2015; 33:1323–32.
17. Shin DS, Park JS, Park HS et al. Outlining of the detailed structures in sectioned images from Visible Korean. *Surg Radiol Anat* 2012;34:235–47.
18. Park JS, Chung MS, Chi JG et al. Segmentation of cerebral gyri in the sectioned images by referring to volume model. *J Korean Med Sci* 2010;25:1710–5.
19. Park JS, Shin DS, Chung MS et al. Technique of semiautomatic surface reconstruction of the Visible Korean Human data using commercial software. *Clin Anat* 2007;20:871–9.
20. Yeom YS, Han MC, Kim CH et al. Conversion of ICRP male reference phantom to polygon-surface phantom. *Phys Med Biol* 2013;58:6985–7007.
21. Spitzer V, Ackerman MJ, Scherzinger AL et al. The visible human male: a technical report. *J Am Med Inform Assoc* 1996;3:118–30.
22. Park JS, Chung MS, Shin DS et al. Sectioned images of the cadaver head including the brain and correspondences with ultrahigh field 7.0 T MRIs. *Proc IEEE* 2009;97:1988–96.
23. Tang L, Chung MS, Liu Q et al. Advanced features of whole body sectioned images: Virtual Chinese Human. *Clin Anat* 2010;23:523–9.
24. Zhang G, Luo Q, Zeng S et al. The development and application of the visible Chinese human model for Monte Carlo dose calculations. *Health Phys* 2008;94:118–25.
25. Zhang G, Liu Q, Zeng S et al. Organ dose calculations by Monte Carlo modeling of the updated VCH adult male phantom against idealized external proton exposure. *Phys Med Biol* 2008;53:3697–722.
26. Cardis E, Armstrong BK, Bowman JD et al. Risk of brain tumours in relation to estimated RF dose from mobile phones: results from five Interphone countries. *Occup Environ Med* 2011;68:631–40.
27. Lee A-K, Hong S-E, Kwon J-H et al. Mobile phone types and SAR characteristics of the human brain. *Phys Med Biol* 2017;62:2741–61.
28. Federal Committee on Anatomical Terminology. *Terminologia Anatomica*. Stuttgart and New York: Thieme. 2002.
29. Shin DS, Park SK. Surface reconstruction and optimization of cerebral cortex for application use. *J Craniofac Surg* 2016;27:489–92.